Resistor–capacitor modeling of the cell membrane: A multiphysics analysis

Christian Brosseau, Elias Sabri

Journal of Applied Physics

RESEARCH ARTICLE | JANUARY 05 2021

Resistor–capacitor modeling of the cell membrane: A multiphysics analysis

C. Brosseau ; E. Sabri

Journal of Applied Physics 129, 011101 (2021)
https://doi.org/10.1063/5.0033608

AIP Publishing

Journal of Applied Physics TUTORIAL scitation.org/journal/jap

Resistor–capacitor modeling of the cell membrane: A multiphysics analysis

Cite as: J. Appl. Phys. **129**, 011101 (2021); doi: 10.1063/5.0033608
Submitted: 17 October 2020 · Accepted: 13 December 2020 ·
Published Online: 5 January 2021

C. Brosseau[a] and E. Sabri

AFFILIATIONS

Univ Brest, CNRS, Lab-STICC, CS 93837, 6 avenue Le Gorgeu 29238, Brest Cedex 3, France

[a]**Author to whom correspondence should be addressed:** brosseau@univ-brest.fr

ABSTRACT

In this Tutorial, we provide a discussion of "What are cell membrane resistance (MR) and capacitance (MC)?" and then give a number of examples to illustrate how cell membranes constitute nature's ultimate stretchable resistor–capacitor network. There are many approaches to the analysis of the electric field effects in cell membranes, but a particularly intuitive and conceptually straightforward method is to use the biophysically inspired lumped parameter resistor (R)–capacitor (C) network in order to simulate the charging and discharging processes. By developing advanced multiphysics and multiscale numerical analysis, we expect to learn many cross-properties of biological materials which involve multiple spatial or temporal scales. These include electrodeformation (ED) and electroporation (EP) biophysical processes occurring in the cell membrane. In a first stage, we present electric and mechanical circuit analog models of cell membranes and examine their predictions and limitations. An important parameter that researchers can tune with these deterministic approaches is the strength of the transmembrane voltage V_m: at low values of V_m, MC varies quadratically as a function of V_m and MR is infinite, but as V_m is increased at a value below the EP threshold, the membrane should be considered as a nonlinear capacitor. Over the EP threshold, there is a decrease in V_m and MR due to the charge transport across the membrane. Mechanical and electrical stresses, singly or in combination, can result in damage and eventually breakdown of the membrane. In a second stage, the parameters in the finite element (FE) modeling that we present are linked to scales we know should be associated with EP and ED processes. We present simulation data and attempt to determine whether the MC and MR behaviors compare well with experimental observations and/or trends from analytical approaches. MC and MR are correlated with the dielectric, mechanical, and morphological information of cells. For an initially spherical cell exposed to an electric field, monitoring MC and MR reflects a quadratic and then higher order nonlinear behavior as a function of V_m. The quadratic regime scales with spheroidal morphologies of the stressed cell up to a critical value of V_m beyond which higher order nonlinearities arise, and the cell shape is no longer described by a spheroid. Furthermore, we consider the present challenges of connecting electrostatic stress, strain energy in multicellular environments to sub-cellular scale material properties, and show that they have the potential to explain the ED and EP of cell membranes via multi-physics and multi-scale numerical analysis. The emergence of V_m as a reporter of neighboring cell interactions is also discussed in a theory-based method for constructing realistic models of tissues based on densely packed environments made by irregularly shaped cells. Of particular interest is the proximity-induced ED and capacitive coupling between neighboring cells, and the subsequent correlation that this has upon anisotropic local ED distribution over a wide range of conditions. For future studies, we identify significant challenges, opportunities, and a sampling of a few used case studies for the development of tissue ED and EP modeling in the coming years.

I. INTRODUCTION

A. Context and motivation

Living organisms are made largely from soft substances that have the ability to stretch and to heal when damaged.[1] Over the years, studies of crowded biological systems (individual cells, tissues, organs, and whole organisms) have revealed a rich phenomenology. The commonality of these systems is that they have complex hierarchical structures that are sensitive to interrelated spatial and temporal dynamics that characterize their internal heterogeneities and are a key part of the physics describing them. It is generally recognized that the progress in biosciences will increasingly depend on deep and broad integration of theoretical analysis into studies at all levels of biological organization. This has

attracted considerable attention over the last few years to model the collective physical (notably, dielectric, and mechanical) response of multicellular systems in suspension or in tissues.[3–7] The study of the cellular hardware (structure and electromechanical properties) and associated cellular software (information processing capabilities) has blossomed into a very active field of research. From an engineering perspective, this also creates an opportunity for biomimetic design: making artificial tissues that can be actuated with an electric field or an extrinsic mechanical stress.

The basic form of the single-shell model of the eukaryotic cell can be traced back to the pioneering paper by Schwan in 1957, which suggested that most eukaryotic biological cells, being highly heterogeneous objects, can be described by the canonical core–shell (CS) structure, i.e., a dielectric nanometric membrane, a phospholipidic bilayer, surrounded by conducting cytoplasm and extracellular medium.[2–3,5,8] Lipid bilayer membranes, i.e., a layer that is only two phospholipid molecules thick, are extremely stable envelopes allowing cells to survive in various environments and to maintain the desired internal composition. The CS models of a biological cell are interesting by virtue of their simplicity from the physicist's standpoint. However, a note of caution is in order at this point. Biological materials are different from standard soft materials due to the fact that they can develop an active response when submitted to stress arising from mechanotransduction, i.e., transformation of an exogenous mechanical stress into a biochemical signal. Although there is an impressive body of experimental data on this phenomenon, direct measurement of MC and MR remains elusive because of the presence of charges at the interface. In a physiological environment, cell membrane surfaces are charged, whether by proteins, like ion channels and enzymes, nucleic acids, like DNA, or most importantly by Na^+, K^+, and Cl^- ions inside and outside cells that screen electrostatic fields over nanometer length scales. Thus, some crucial questions cannot be answered with available experimental techniques.

An electric field interacts with the molecular polarizability to generate forces, torques, and internal stresses. One problem is that we need to take into account the electrodeformation (ED) and electroporation (EP) of cell membranes that are often poorly known, and therefore, the underlying physical processes of creation and evolution of pores in the membrane can be problematic to simulate.[9–15] As a result, it remains difficult to understand the distribution of forces within a cell membrane. In fact, there are two questions: When a cell is exposed to a uniaxial electric field, how MC evolves when its morphology is changed (ED and EP)? and a subsidiary theme is, how an increase in the transmembrane voltage can potentially affect the membrane dimension (electrostriction EL)? The answer to these questions is of interest, for example, in dielectropheresis studies of biological cells,[16,17] and when one wants to know how a living cell exchanges information with its surroundings, which requires understanding how materials pass through the cell membrane. Several studies have shown that the dielectric properties of cells are determined by the difference in cell membrane morphological complexity.[18,19] While elegant, this technique has proven to be especially challenging for two reasons: it needs performing SEM imaging of cell specimens composed of homogeneous single-shell cell suspensions. The second reason lies in the peculiarities of cell rheology; in particular, it remains difficult to get an in-depth understanding of the mechanical properties of cells; i.e., how changes in the cellular shape can occur in response to environmental cues? The mechanical properties of cells are largely determined by the cytoskeleton network, a hybrid polymer gel consisting of several kinds of different filamentous proteins, consisting of filamentous actin (F-actin), microtubules, and intermediate filaments, whose primary function is to give the cell its shape and mechanical resistance to deformation. Microtubules have unique electrical properties because of their distribution of charges and large dipole moments. Thus, microtubules may affect their interaction with the surrounding molecules beyond the short-range Coulomb and van der Waals interactions.[20] Since the cytoskeleton interacts with the cell membrane, it is reasonable to assume that it may affect the ED and EP processes.

This is also compounded by the fact that conventional measurements, such as cytoplasmic rheology, blend the response of these complex materials, exhibiting a high degree of structural hierarchy and heterogeneity and provide only a homogenized comparison for modeling efforts.[21] Yet, natural tissues are structurally complex and composed of multiple cell types. Indeed, it is only recently that computer models have shed some light on simultaneous ED and EP models of tissues[7,9,22,23] and have renewed interest in the problem, but a direct investigation of the spatiotemporal processes of creation and evolution of pores on the nanometer level, i.e., 20–120 nm, is still lacking. Multiphysics and multiscale analysis of materials that can perform interactions across several characteristic lengths and timescales is an emerging area that has gained attention in recent years.[24–26] Understanding how and to what extent these electromechanical changes induce and influence MC and MR would provide an improved physical description of biological systems and help isolate the role of specific factors based on their influence on MC and MR. One efficient tool for addressing such questions is a heuristic mathematical model based on an electric RC circuit equivalent model, built so as to capture the transient dynamics associated with charging and discharging the membrane, respectively.[27–29] As was pointed out by many authors, these models also constitute a source for well-grounded assumptions for empirical studies of the ED of cell membranes.[30–42] Over the years, a lot of material has accumulated on the standard linear solid (SLS), also known as the Zener model, which is a method of modeling the behavior of a viscoelastic material using a linear combination of springs and dashpots to represent elastic and viscous components, respectively.[38,43] Mechanical relaxation under the constraint of biological materials is concomitantly enjoying growing interest.[44] Two types of modeling approaches are primarily used to study EP. On the one hand, the molecular dynamics (MD) based first-principles simulations of defect formation are useful to describe processes during pore formation at a small spatial, i.e., nanometers, and timescales, i.e., picoseconds to nanoseconds.[45–47] Although conceptually compelling and computationally expensive, these models leave open the question of quantitatively determining molecular uptake. Another strategy is based on continuum partial differential equations and use FE for solving boundary value problems.[7,9,22,23,48–52] These continuum theories rely on the idea of smearing out the underlying discreteness of matter with continuum scalar and vector field variables. FE is a very efficient and popular way to computationally solve Maxwell's equations for studying the

TABLE I. Predictions of physical quantities or physical behaviors by different theoretical approaches for a single cell.

Physical quantity Type of model	Membrane capacitance C_m and resistance R_m	Transmembrane voltage V_m	Spatial distribution of the electric potential, pore density	Dynamics of pore formation and evolution	ED and dynamic electromechanical behavior
Electrical and mechanical circuit equivalent models[53–59]	✓			✓	✓
Electromagnetic analysis[4,5,19,25,27]	✓	✓	✓		
FE modeling [7,9,22,23,48–52]	✓	✓	✓	✓	✓
MD simulation[45,46]				✓	

interaction of matter with fields. This adds flexibility for modeling the membrane response to much longer electric stimulation (from microseconds to milliseconds), making it relatively easy to explore all types of voltage and strain rates. Such spatiotemporal modeling has the advantage of connecting quantitative cell-level behavior with cell assembly-level phenomena.[7,9,22,23] In Table I, we compare the predicted physical quantity from these previous computational studies. As an aside comment, it is also noticeable that well before humans carried out EP experiments, nature may have used it due to lightning strikes into the sea and land, to fuse and transfect microorganisms.[41]

So, many papers have cluttered up the archival literature that it seems necessary to write a progress report-type paper on where we have gotten so far, i.e., the things that could be agreed as a basis for further work. This article aims to provide a current landscape of the field of MC and MR as well as to illustrate relevant opportunities and challenges. Aiming to facilitate the understanding of the field to non-experts, we overview the principles, practices, and perspectives of cell membrane electromechanobiology. Our primary interest in this paper is to present the intricacies of the biophysically inspired lumped parameter RC equivalent circuit model for describing a simple continuum model of cells.[53–59] Our other motivations are to analyze FE predictions of the transmembrane voltage, MC and MR, and compare the results with those obtained from RC analysis. This allows a convenient examination of the electric behavior of the cell membrane in an electromechanically coupled material system. Ultimately, one of the primary ways of checking a model lies in the ability to make predictions about as-yet undone experiments. The developments of earlier studies on membrane ED and EP make it possible to examine the question of whether available experimental data are well reproduced by theory. Another question that would benefit from direct investigation is the possibility of defining precisely a metric based on MC and MR which can estimate the critical transmembrane potential at which EP is initiated. A technology that would simultaneously record TMP and encoded TMP indicators such as MC and MR will have a transformative effect on ED and EP cell research.

B. Structure of this paper

Our approach in this paper is to first present in Sec. II the general notations to familiarize the reader with the basic concepts and briefly review isolated cell models with time-invariant, static and passive membranes, i.e., the kind of insight that can be discussed on a blackboard. We then proceed to describe lumped parameter RC circuit models. There are impressive approaches in which the properties of the membrane are modeled using RC networks. We illustrate their main features with typical examples for ED and EP membrane purposes. In Sec. III, we report the results from FE simulations of the electromechanical properties of biological cells which are carried out for different cell configurations and electric stimulations. This will allow us to consider an efficient and versatile numerical method for constructing realistic theory-based tissue models of irregularly shaped cells in proximity, analyze membrane electromechanics, and quantify the cell MC and MR variation as a function of both V_m and neighboring cell proximity. Finally, in Sec. IV, we present our conclusions and discuss opportunities for the future.

II. BACKGROUND AND NOTATIONS: A CORNUCOPIA OF IDEAS

The objective of this presentation is to provide some basic examination and analysis of the dielectric and mechanical responses that are observed for cells in suspensions. The intended scope of the remarks includes both the interpretation of experimental data and the relevance of simple physical models intended to interpret these data. For the present purposes, only a few of the primary concepts will be examined. We will ignore all the complexities of the biochemistry machinery found inside the cell (e.g., cytoskeleton, Golgi apparatus, nucleus, etc.) and outside the cell (e.g., adhesion between neighboring cells, etc.) and simply consider the membrane as a little bag filled with saline, i.e., water with ions dissolved in it.

A. Transmembrane voltage

As mentioned above, the membrane of eukaryotic cells is composed of a flexible lipid bilayer. The transmembrane voltage V_m is the difference in voltage between the interior and the exterior of a cell and arises from the interaction of ion channels and ion pumps embedded in the membrane, which maintain different electric charge carrier concentrations on the intracellular and extracellular sides of the membrane. In their physiological state, the membrane potential of non-excited cells is called the resting

potential V_{rest}, i.e., reflecting the imbalance of electrical charge that exists between the interior of biological cells and their surroundings. The value of V_{rest} is determined by the concentration gradients and the relative permeability values of ions for which there are open channels in the membrane, i.e., Goldman–Hodgkin–Katz equation.[19] The surface of a cell membrane in an aqueous environment becomes negatively charged. Thus, a thin double layer of mobile cations is accumulated adjacent to the extra-intracellular membrane surfaces.[8,19,60] Its magnitude varies according to cell type, but the inner surface is always more negatively charged than the outer one, and the magnitude of V_{rest} is roughly -0.07 V,[4,29,38,54–56] leading to an electric field of the order of $10^7\,\text{V m}^{-1}$. Additionally, V_{rest} is constant everywhere on the cell membrane. Opening or closing of ion channels at some specific point in the membrane produces a local change in V_{rest}, which causes electric current to flow rapidly to other points in the membrane. Distinct from the effects of external electromagnetic field exposure, it is now known that the endogenous gradients of voltage serve as signals regulating cell proliferation, differentiation, and migration.[58] When an external electric field E is applied to the cell, the induced transmembrane voltage (ITV) V_m superimposes to V_{rest}. It results in a broad range of effects depending on the electric field intensity and the duration of its application. It is commonly understood that the value of V_{m} dictates the onset of pore formation, i.e., when $V_{\text{m}} > V_{\text{EP}}$. Experimental estimates for V_{EP} fall in the range of 0.2–1.5 V,[41,50,55–58] so the huge electric field strength across the membrane is on the order of $10^8\,\text{V m}^{-1}$ (compared with the $3\ 10^6\,\text{V m}^{-1}$ fields associated with atmospheric lightning). As the number of pores increases, the membrane conductivity σ_m (respectively the membrane resistance R_{m}) increases (respectively decreases) until critical pore size and number are attained,[61–65] which have, for effect, to counteract the V_{m} increase. A visualization of isolated pores by fluorescence imaging during the application of potential allows an estimation of their conductance, typically 400 pS, in support of the hydrophilic pore model.[59] The long history of scientific and technological interest in EP and ED has generated an enormous phenomenology presented partly in the approximate electric pulse strength-duration space diagram shown in Fig. 1, which involves seven orders of magnitude in duration and three orders of magnitude in strength.

A closer look at Fig. 1 shows that ED is not considered in this diagram. It should be emphasized that this phenomenon eventually impacts the threshold values displayed here since it is widely recognized that membrane cells can react and adapt to electromechanical stresses.[9] However, the absence of an in-depth understanding of the physical mechanisms by which the MC and MR vary as V_{m} is increased renders the identification of the physical parameters and behaviors that control the EP of a deformable membrane speculative.

B. MC and single-shell model

A biological cell contains highly conductive (material parameters are typically for cytoplasm: $\sigma_c \approx 0.3\,\text{S m}^{-1}$ and relative permittivity $\varepsilon_c \approx 60$; extracellular medium: $\sigma_e \approx 1.1\,\text{S m}^{-1}$ and relative permittivity $\varepsilon_e \approx 76$) aqueous electrolytes separated by a very thin, low-conductivity membrane ($\sigma_m \approx 10^{-5}\,\text{S m}^{-1}$, relative

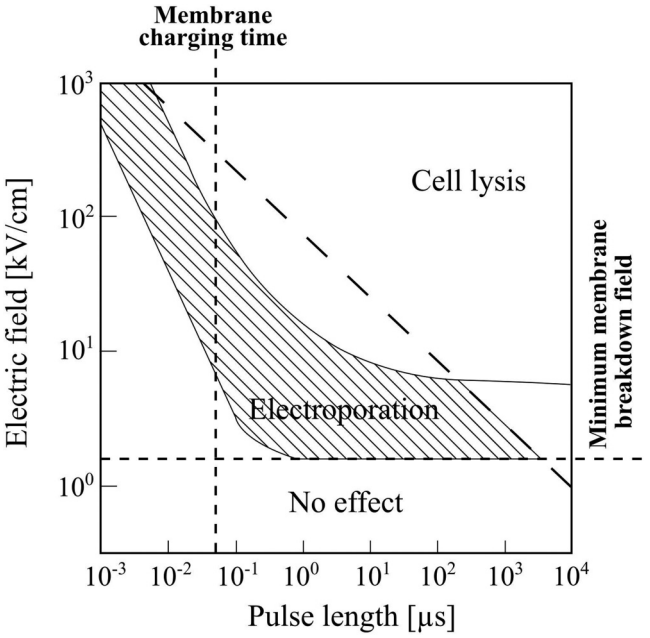

FIG. 1. Schematic diagram of the electric pulse strength-duration space with important examples of electric field effects in biological systems ranging from E D, including reversible or irreversible EP and membrane disruption. Typically, when a biological cell is subjected to an electric pulse of magnitude above a few kV cm^{-1} and duration in the range of μs-to-ms, numerous hydrophilic pores are formed in the membrane, which becomes permeable (hatched region). Strong electric pulses of short duration induce electric breakdown in membrane integrity. Breakdown leads to the formation of transient pores occurring on the order of ps-to-ns. In the minutes to hours following EP, a porous membrane can reseal to again inhibit molecular transport. At a very large pulse duration, the reversible breakdown turned into an irreversible mechanical breakdown, associated with the destruction of the membrane, i.e., the cell cannot regain its homeostasis after EP, eventually leading to cell apoptosis [adapted from Weaver *et al.*, Biolectrochemistry **87**, 236–243 (2012). Copyright 2012 Elsevier].

permittivity $\varepsilon_m \approx 11$, and thickness $d \approx 5$ nm). Within a simple electrostatic model, the cell membrane can be considered as a capacitor that can be charged by applying a field across the membrane. Electrically speaking, the membrane can be considered as a capacitor separating two conductors. The capacitive nature of the membrane is essential for cell viability in external fields, because it acts as a shield to the cytoplasm. The conventional equations describing electrostatic effects in a biological cell predict proportionality between the total charge Q_m accumulated at the inner and the outer surfaces of the membrane and V_m, i.e., $Q_m = C_m V_m$. An implicit, yet fundamental, assumption underlying membrane electrical modeling is that it can be described by a parallel-plate capacitor made with two identical plates. The capacitance with plate area A_{m} and thickness $d_m \ll A_m$ is $C_m = \frac{\epsilon_0 \epsilon_m A_m}{d_m}\left[1 + O\left(\frac{\log\left(\sqrt{A_m}/d_m\right)}{2\sqrt{A_m}/d_m}\right)\right]$.[65] Thus, its capacitance per unit area is $\tilde{C}_m = \varepsilon_0 \varepsilon_m / d_m$since the second term in the brackets can be ignored. Typical data obtained on biological cells indicate

that the MC per unit area is of the order of 10^{-2} F m^{-2}, which represents a very large capacitance per unit area because of the nanometric thickness of the membrane.[2,8,65–67] The larger the area, the larger the capacitance will be. Keep in mind that the membrane has also an associated areal resistance of the order of $10^{-2}\,\Omega\,m^2$. Assuming a uniform permittivity in the membrane, the field across the membrane is $E_m = V_m/d_m$, and the force acting on this capacitor is $F_m = C_m V_m^2/2d_m$. This results in a pressure on the membrane of 10^4 N m^{-2} at 100 mV (voltages close to 100 mV are typical in the voltage clamp electrophysiology experiments used to measure protein conductance). This pressure has a direction normal to the membrane surface. This implies that increasing the force results in a reduction of thickness and an increase of area. Additionally, the membrane resistance value is in the range 10^9–$10^{11}\,\Omega$.[4,8,38,66] These values have been repeatedly confirmed experimentally. Consider a spherical cell of radius $R = 10\,\mu$m, which represents a surface area $4\pi R^2$ of typically 10^{-9} m^2, actual MC of the order of 10 pF, and actual resistance $10^9\,\Omega$ at low values of V_m. If one sets V_m to 5 mV, this would require a charge transfer of 1.6 10^{-14} C across the membrane, i.e., corresponding to 9.8 10^4 univalent cations (each bearing an elementary charge of 1.6×10^{-19} C). If the cytoplasm is modeled as a physiological solution (0.10 N) KCL containing 3×10^{10} univalent K^+, it means that the generation of a voltage difference across the membrane of 5 mV necessitates the change in the number of K^+ of 3 ppm. This illustrates the strength of the electric effects, i.e., the membrane has a very large capacity to store charge with little voltage rise. MC may also change due to local membrane thickness variations at lipid rafts, which are 10% thicker than non-raft membranes.[38]

A couple of notes are in order. First, it is worth mentioning that the MC and MR are measurable quantities in the entire biologically relevant frequency range, i.e., from dc to say 100 MHz by impedance spectroscopy techniques.[51] Second, Everitt and Haydon[52] proposed an interpretation of the MC of a lipid membrane (uniform thickness, infinite MR, and uniform surface charge density) separating two aqueous phases by considering its surface charge density, electrolyte concentration, and applied potential. The capacitance per unit area was given as $\frac{1}{C_m} = \frac{4\pi d_m}{\varepsilon_0 \varepsilon_m} + \frac{8\pi}{\varepsilon_0 \varepsilon_c \eta}$, where the first term represents the standard geometric capacitance and the second term corresponds to the planar electrical double layer contribution (η is proportional to the Bjerrum length, which is defined as the separation at which the electrostatic interaction between two elementary charges is comparable in magnitude to the thermal energy scale and to the electrolyte conductivity). From this expression, we observe that the electrical double layers contribute only weakly to the MC since the right term represents only 1% of the total MC for Bjerrum lengths within physiological bounds (a few nm) and electrolyte conductivities above 5 mS/m (which is around 3 orders of magnitude lower as compared to typical buffer conductivities used in EP experiments).

A note of caution must be added here. First, it should be stressed that the relative permittivity of the membrane and the surrounding aqueous electrolyte are not spatially uniform.[25] In other words, in the hydrophobic region of the lipid tails, the relative permittivity is very small, while in the region of lipid headgroups, it is decreasing in direction from the outer solution toward the boundary between the hydrophilic and the hydrophobic part of the lipid bilayer.[67] The local fluctuations of permittivity are not taken into account in the analytical expression of MC. Second, the consideration of the membrane as a capacitor separating two conductors represents a simplification if one would like to describe the membrane electrostatics in details. The differential capacitance of the electric double layer on both sides of the membrane may be strongly influenced by the different conditions in an electrolyte solution, e.g., the finite size of ions, asymmetry in the size of the ions, etc.[67]

C. Cell (single-shell) modelization by an RC circuit equivalent model

Figure 2 provides the starting point. An important problem in using a RC model for describing the ITV is the calculation of the membrane charging time τ_m as a function of the RC characteristics. One way to formalize what might be going on here is to take advantage of the quasistatic approximation since $2\pi\varepsilon_{c,e}\varepsilon_0/\sigma_{c,e} \approx 10^{-9}$ s and $2\pi\varepsilon_m\varepsilon_0/\sigma_m \approx 10^{-4}$ s, where F and ε_0 denote the frequency of the (harmonic) electric field and the vacuum permittivity, respectively, and the displacement currents in the cytoplasm and in the extracellular medium are negligible compared with the conduction current (typically below 100 MHz), i.e., the electromagnetic field cannot distinguish the details of the cell, which can be described by an effective medium.[24] Then, the (spherical) cellular dielectric properties can be described by an equivalent RC network, i.e., coarse-grained modeling of materials. In the following, only DC stimulation (steady-state or pulse) is considered.

The mathematical formulation of this problem consists in solving Laplace partial differential equation which considers continuous spatial and time variations of every physical quantity in the cell for a dc homogeneous electric field E excitation in order to get the internal and external potentials. Dirichlet conditions are dealt with only at cell boundaries. The cytoplasm and the extracellular

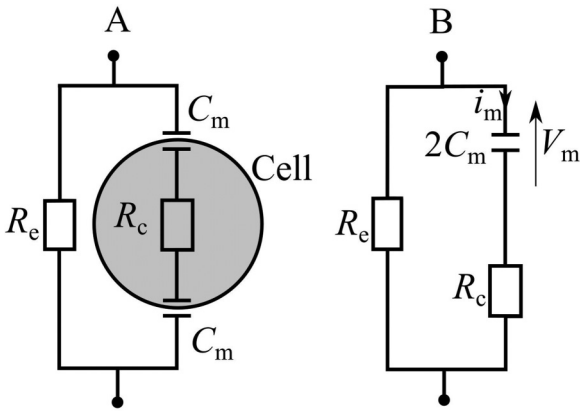

FIG. 2. (a) A cross-section schematic diagram illustrating an RC configuration of the (single-shell) CS structure of an idealized spherical biological cell of radius R. (b) The membrane, of uniform thickness, is considered as passive (the ideal capacitor presumption leads to a nominally infinite resistance of the membrane, i.e., σ_m can be considered as negligible compared with σ_c and σ_e).

medium can be described by resistors, i.e., R_c and R_e, respectively, and the membrane can be described by C_m (R_m is infinite). If the membrane is electroporated, a variable resistance is added to model the resistance decrease due to the pore formation (typically from an initial value of $10^9\,\Omega$ to a few $10^2\,\Omega$). Several tacit assumptions need be considered. First, the cytoplasm is treated as a single-phase material. Second, the intact (nonelectroporated) membrane is purely capacitive. Third, the membrane is considered as a rigid object with a smooth surface. Fourth, the cytoplasm and the membrane are perfectly concentric (uniform membrane shell) spheres. Fifth, all permittivity and conductivity values are time-invariant. Sixth, at time $t = 0$, the external uniform electric field (e.g., microsecond pulse) is provided by infinitely distant electrodes.

Thus, we get Schwan's equation,[2,] i.e., the ITV is $V_m(t,\theta) = \frac{3}{2}ER\cos\theta\left(1 - \exp(-\frac{t}{\tau_m})\right)$, where $\tau_m = \frac{R\tilde{C}_m(\sigma_c+2\sigma_e)}{2\sigma_c\sigma_e}$ denotes the time constant for membrane charging, and θ denotes the angle between the surface normal and the field direction. The value of τ_m is found to be in the range 0.1–1 μs at physiological conditions (Fig. 1) for a 10 μm cell, meaning that if τ_m is small compared with the duration of E, a convenient simplification occurs, and Schwan's equation is $V_m(\theta) = \frac{3}{2}ER\cos\theta$[68] expressing a linear dependence of V_m on the cell radius R. This is also consistent with the fact that a much stronger electric field magnitude has to be applied for ns EP (Fig. 1), because, in this situation, the pulse duration is too small for the membrane charging to complete. Most of the potential drop across the cell is effective across the membrane. As a result, the cytoplasm is shielded from the applied field. During electric field stimulation, the electric current density through the cell membrane is obtained by summing the capacitive current $\left(\tilde{C}_m\dot{V}_m(t)\right)$ and the conduction current $(\sigma_m(V_m + V_{rest})/d_m)$, where $V_m + V_{rest}$ is the overall transmembrane voltage. It is worth noting that unlike V_{rest} which is constantly present in the cell membrane, the ITV varies with position over a cell membrane according a cosinusoidal shape, i.e., $V_m(\theta) \propto \cos\theta$: a spherical cell will polarize in such a way that the maximum and minimum of the overall V_m occur at the poles of the cell and are equal to V_{rest} at the equator. However, this analysis cannot reproduce the flattening of V_m observed in electroporated membrane regions, i.e., at the poles.[6,28,68] Beyond V_{EP}, V_m cannot be further increased, and can even decrease due to the charge transport into the membrane.[68] Unfortunately, the above derivation is valid only for regular cell shapes. In three-dimensions, the best we can do for realistic cells is to solve the Laplace equation by using numerical methods; see, e.g., Refs. 4, 6, and 9. Additionally, Schwan's equation does not hold for short electric pulses, i.e., well smaller than τ_m, for which the pulse duration and repetition are parameters of paramount importance for estimating V_m.[4,7,58,63]

D. ED and transmembrane voltage-dependence of membrane capacitance

As discussed in the above formulation, it was assumed for simplicity that the membrane capacitance C_m is constant. Now, we address issues related to the ITV dependence of C_m where we need to account for the fact that charges on a capacitor generate mechanical forces, i.e., Maxwell stress tensor.[27,38,65,70] A nice synopsis of the field of electromechanics is discussed in Ref. 17. By way of consequence, these forces can change the dimensions of the capacitor, e.g., d_m decreases, and the capacitance C_m increases. Hence, we expect a nonlinear behavior of the MC as V_m is increased. Classical EL theory allows us to provide a crude estimate of the magnitude of the force on a membrane, which is a quadratic function of voltage when the membrane is polarized. Assuming a membrane with constant area and small thickness change, Mosgaard and co-workers[70] suggested that the capacitance is proportional to the force and can be described as a quadratic function of voltage. Based on experimental data on artificial bilayer membrane, Alvarez and Latorre[71] demonstrated that the dependence of MC on V_m can be written as $C_m = C_{m0} + a'(V_m - V_{rest})^2$, where $C_{m0} = C_m(V_m = V_{rest})$ and a' denotes a fitting parameter. Heimburg suggested that the change in C_m can be expressed as $C_m = C_{m0}(1 + \chi V_m^2)$, where χ is a constant (close to $10^{-2}\,V^{-2}$) and should be attributed to EL, i.e., an increase in A_m and a decrease in d_m.[72]

Multiple RC configurations in the time domain have been proposed[73–75] for describing the pre-transitional state of ED of the membrane underlying the EP phenomenon. The majority of the current literature on RC models is focused on characterizing ionic currents through different porosity stages and does not consider relevant spatial scales, e.g., d_m. An illustrating example is shown in Fig. 3, where the authors developed a model that describes the cellular electro-viscoelastic membrane based on thermodynamic principles.[73] Within this analysis, it should be realized that the presumption of a pure capacitive membrane is relaxed, but the MC and MR are constant.

These ideas have motivated a lively collection of RC circuit equivalent models. Further details and a discussion of these efforts can be found in Refs. 74 and 75. Several authors, e.g., Refs. 77 and 78, have also argued that the increase of MC is related to the sphere-to-spheroid transformation, i.e., surface expansion of the

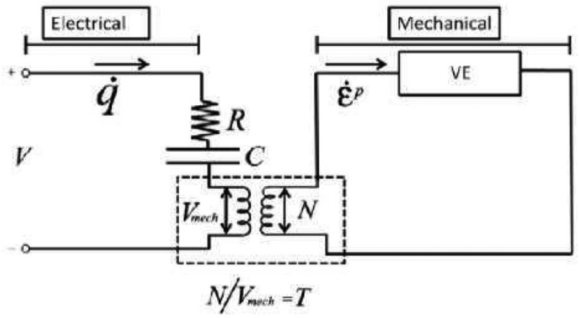

FIG. 3. RC circuit equivalent model of the ED and the electromechanical coupling in a cell membrane. The left panel represents the electrical circuit where *V, R, C,* and *q* denote, respectively, the membrane voltage, MR, MC, and the rate of the transferred charge (current). The right panel represents the mechanical part of the model, where $\dot{\varepsilon}^p$, V_{mech}, *N*, and *T* stand for the rate of passive strain, mechanical component of the voltage, membrane resultant, and the transformer ratio, respectively Reproduced with permission from Roy *et al.*, PLoS ONE **7**, 37667 (2012). Copyright 2012 Author(s), licensed under a Creative Commons Attribution (CC BY) license.

membrane of an initially spherical cell exposed to the electric excitation as V_m is increased. Notice that this statement is completely consistent with experimental observations that have been made in many places, e.g., Ref. 77. In mechanical equilibrium, the degree of stretching can be estimated by the aspect ratio b/a, where b and a are the two principal semiaxes along and perpendicular to the electric field direction, respectively. A prolate spheroid (of revolution) has a surface area defined as $2\pi a^2 + 2\pi ab\sin^{-1}(e)/e$ with $e = \sqrt{b^2 - a^2}/b$. The maximum deformation corresponds to about 10% in terms of aspect ratio[9,22,77] and is expected to depend on the initial surface tension of the membrane and the excess area of an initially spherical cell of the same volume, $\delta A_m/A_{m0} \cong \ln(\Gamma/\Gamma_0)kT/8\pi K$, where A_{m0} is the initial surface area for which the tension is Γ_0, Γ is the membrane tension when the cell is exposed to the electric field, K is the membrane bending stiffness ($K \cong 10^2$ kT), and kT is the scale factor for energy. Needham and Hochmuth considered that V_m induces a Maxwell (electrocompressive) stress tensor on the membrane that manifests as an additional membrane tension (MT) that is proportional to V_m^2.[78] MT relates to cellular phenomena that induce membrane shape changes at constant volume resulting in a molecular scale shifting of membrane lipid equilibrium configuration, giving rise to tension within the membrane that cannot exceed the lysis tension (Fig. 1).

But although there has been a good deal of attention directed toward probing different RC circuit equivalent models to analyze ED, relatively little exploration has been dedicated to studying EP because of the no-scale structure of these models. Furthermore, the possibility of such electrical circuit equivalent models for describing the membrane ED at large values of V_m, the membrane EP, and the collective behavior of cell clusters (tissues) raises a group of open questions, e.g., do these models produce representative electrical waveforms that can be checked out with measurable signals?

E. EP and cross membrane transport of small molecules

We can begin to ask why EP is a thresholdlike phenomenon.[76,77] This means that EP takes place when V_m exceeds a threshold V_{EP} above which electrically conductive (hydrophilic) nanopores start forming in the membrane. The literature suggests several ways to deal with this issue and also provides estimates of V_{EP}. Such estimates do suggest that dynamically formed pores in membrane could contribute significantly to observable events. The pores are primarily formed where the local electric field is maximal and expands in size if the electric field is sustained until critical pore size and number are attained.[79]

Reversible EP occurs when the MT reaches a critical magnitude. Supercritical MT can also result in lysis (accompanied by irreversible EP), with reference to Fig. 1.[30–36] To address this issue, Needham and Hochmuth[78] argued on the basis of simple back-on-the-envelope calculation of the storage of elastic energy in a flat incompressible membrane at equilibrium as a result of work done at the boundaries of the system by either tensile or electrocompressive stress, that the tension in the membrane takes the form $\Gamma = A\delta A_m/A_{m0} - \tilde{C}_m V_m^2/2$, where A is a specific constant and $\delta A_m/A_{m0}$ denotes the relative increase in the surface membrane area. Then, a general failure criterion of a membrane is suggested when $\Gamma = 0$, i.e., $V_m^c = \sqrt{2A\delta A_m/A_{m0}\tilde{C}_m}$, providing a critical membrane voltage required for breakdown. Needham and Hochmuth[78] conducted a series of electromechanical experiments for three kinds of membrane systems (artificial lipid bilayers) and showed that this relation is verified experimentally for 50-μs pulses. The tricky thing is that we do not know *a priori* if this analysis gives us the correct EP condition, i.e., $V_{EP} = V_m^c$.

An important parameter that the researchers can tune in addition to the voltage strength is its pulse duration. Akinlaja and Sachs[80] attempted to determine whether mechanical tension and electric couple stress too cause breakdown in cells. In their experimental work dealing with HEK293 cells, voltage pulses of increasing amplitude were applied until the authors observed a simultaneous sudden decrease of R_m and increase of C_m. Complicating this interpretation, they found that the mechanisms of high field/short pulse and low field/long pulse breakdown are fundamentally different: for pulses of 50 μs duration, the breakdown required >0.5 V and was dependent of the tension, whereas for pulses of 50–100 ms duration, the breakdown required 0.2–0.4 V and was independent of tension. Reference 80 also identified that the critical energy (voltage) underlying the EP criterion cannot be compared with experimental data without a model that incorporates time.

When $V_m = V_{EP}$, typically in the range from 0.2 to 0.6 V when V_m exists for times of about 100 μs or longer (Fig. 1), then electrical breakdown and destructive rupture of the membrane manifest as a very rapid drop in R_m. This can be explained by the large population of transient pores in the membrane. Having identified the critical nature of EP, we now attempt to gain further insight into understanding the physical framework that aims to capture the electromechanical behavior of membranes and link this to the creation of pores in the membranes by the transition over an energy barrier due to thermal fluctuations as V_m is increased.[59] Figure 4 illustrates such a model for which the kinetics of pore formation is described by the transition over an energy barrier created by the intersection of two different pore configurations, namely, a hydrophobic pore where the lipid phase is broken up and a hydrophilic toroidal pore [Fig. 4(a)]. For small radii, the hydrophilic pores are confined within a local energy minimum, while for large radii, there exists a local maximum beyond which a pore may grow indefinitely. The free energy of the hydrophilic pore is changed upon application of ITV such that its free energy, along with this local maximum, is decreased [Fig. 4(b)]. At some critical potential, the local maximum restraining pore expansion vanishes and the pore grows until the bilayer is destroyed.[59]

Furthermore, under an electric field stimulation, it is reasonable to predict that electropores appear and disappear in the membrane in a stochastic manner and have fluctuating sizes. The transient nature of electropores places significant limitations on the characterization of their dynamics. Recently, Ref. 59 provided an improvement in our experimental understanding of electroporation by imaging individual voltage-induced defects in a bilayer membrane by detecting a fluorescent signal proportional to the flux of Ca^{2+} flowing through a pore. Using optical single-channel recording, Sengel and Wallace[59] were able to track multiple isolated electropores in real time in planar droplet interface bilayers (formed from the contact between an aqueous droplet and a hydrogel

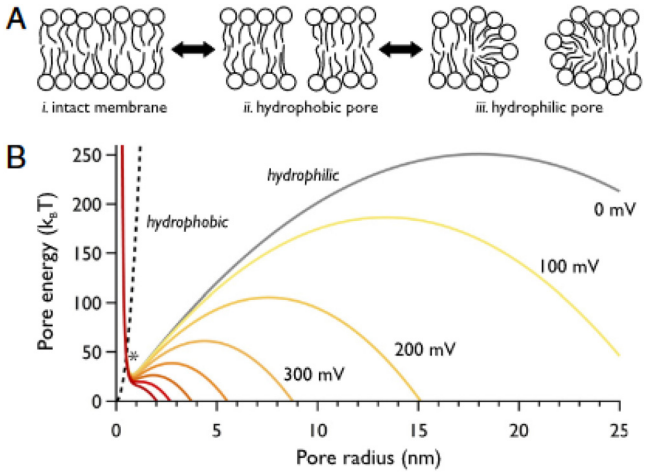

FIG. 4. (a) Illustrating the transient aqueous pore hypothesis for the purpose of understanding EP, the pore energy $U(r,V_m)$ is defined as $U(r, V_m) = -\frac{1}{2}\tilde{C}_m V_m^2 \pi R^2 + 2\pi R - \Gamma R^2 + (\frac{\beta}{R})^4$ (each term from left to right is being respectively associated with the release of electrostatic energy, linear tension, surface tension, and lipid head steric repulsion contributions). A sequence of lipid bilayer rearrangements leading from the unperturbed membrane (i) to the formation of a non-conducting hydrophobic pore (ii) to the creation of a hydrophilic pore (iii); (b) The dashed (respectively solid) line represents the hydrophobic (respectively hydrophilic) pore free energy. The numbers denote the ITV values. Reproduced with permission from Sengel and Wallace, Proc. Natl. Acad. Sci. U.S.A. **113**, 5281–5286 (2016). Copyright 2016 PNAS Publishing.

surface immersed in a phospholipid/oil solution). They observed individual mobile pores that fluctuate in size and with a range of dynamic behaviors revealing complexity in their interaction and energetics. Furthermore, their observation is consistent with the fact that the potential well that supports hydrophilic pores (Fig. 4) widens and shifts to larger radii when ITV is increased.

Stabilization of hydrophilic pores can be also realized by heterostructures contained in the membrane. We further observe that due to the highly unfavorable line tension of the pore rim, membrane pores are generally not expected to be energetically stabilized. Fošnarič and co-workers described a theoretical model that predicts the existence of stable pores in a lipid membrane, induced by the presence of anisotropic inclusions.[81] Furthermore, they argue that the optimal pore size is governed by the shape of the anisotropic inclusions, i.e., saddle-like inclusions favor small pores, whereas more wedgelike inclusions give rise to larger pore sizes.

Cross membrane transport refers to ion or molecule transport across the electroporated membrane through aqueous pores. Based on minimization of the membrane energy, Barnett and Weaver[55] proposed an asymptotic Smoluchowski model to describe the creation, destruction, and evolution of cylindrical pores, which was later modified by Neu and Krassowska.[54] On the basis of coarse-grained descriptions of the membrane, several groups concluded that cell EP can be described by the formation of hydrophilic pores in the membrane; see, e.g., Refs. 45 and 82, resulting in a significant increase of σ_m and current density across the membrane, namely, $j_m(t) = \sigma_m(V_m + V_{rest})/d_m + \tilde{C}_m \dot{V}_m(t) + j_{EP}(t)$, where j_{EP} denotes the current density flowing through the pores.[85] An expression of j_{EP} based on the Nernst–Planck equation was suggested as a function of V_m.[84–86] It was shown that one can extract information about pores by solving an evolution equation that governs the dynamics of the pore density per area as a function of their radius and time t, $\dot{N}(t) = \alpha \exp((V_m/V_{EP})^2)[1 - (N/N_0)\exp(-q(V_m/V_{EP})^2)]$, where N_0 is the pore density in the unelectroporated membrane, and α and q are two parameters encoding the EP process. Since this model relies on the exponential of the squared ITV, it requires small time steps to resolve in numerical simulations. For derivations of this expression and comprehensive discussions of the underlying theory, the reader is referred to Refs. 58 and 84. Within this model, one assumes that all identical non-interacting pores have reached their equilibrium size before the end of the electric pulse for μs EP, since the pulse length is much larger than the characteristic timescale of pore evolution.[54,55]

There has been much effort directed to develop energy-based EP models[53] in order to predict the EP activation energy, V_{EP}, and the equilibrium pore size. First, consider the membrane as an infinitely thin film without internal structure subjected to external lateral tension σ, i.e., this would correspond to the situation for which $V_m = V_{ext}$. The energy of a cylindrically symmetric pore with radius r can be written using Derjaguin's equation,[87,] i.e., the work required to create a pore in the cell membrane, at $V_m = 0$, is given by $U(r) = 2\pi\gamma r - \pi\Gamma r^2$, where γ is the edge energy density of the pore ($\gamma \cong 10^{-11}$ J m^{-1}) and Γ is the membrane surface tension ($\Gamma \cong 10^{-3}$ J m^{-2}). The system energy has a maximum at critical radius $r_c = \gamma/\Gamma$ defining the energy barrier to pore formation $U(r_c) = \pi\gamma^2/\Gamma$. Pores with $r < r_c$ are reversible and tend to close, whereas those with $r > r_c$ grow unlimitedly, eventually causing membrane breakdown.[88] Now, consider that a source current proportional to the exogenous electric field drives an increase in V_m beyond V_{EP}, thus membrane defects begin to occur. The pores, assumed to be cylindrical (radius r), are estimated to require energy $U(r, V_m)$ to be created by thermal fluctuations, where $U(r, V_m) = -\frac{\pi}{2d_m}(\varepsilon_e - \varepsilon_m)V_m^2 r^2 + 2\pi\gamma r - \pi\Gamma r^2$, where again the first term accounts for the drop in the electrostatic energy stored in the membrane induced by pore formation; the second, for the line tension acting on the circumference of the pore; and the third, for the surface tension of the membrane. In like fashion as above, this free energy form leads to a critical pore size at which the energy reaches an activation energy.[54,55,85] In this case, the system energy has a maximum at critical radius $r_c = \gamma/(+\tilde{C}_m V_m^2/2)$. Within this approach, the rate of change of the pore radius is determined by $\dot{r} = -\frac{D}{kT}\frac{\partial U(r)}{\partial r}$, where D is the diffusion coefficient of pore radius,[53,82] i.e., a pore must be thermally activated to overcome the nucleation activation energy. The pores expand in size with time if the electric field is sustained until an unstable pore size is reached, e.g., up to 50 nm.[61,79] This model predicts that the electric pulse produces more but smaller pores on the hyperpolarized cell hemisphere and fewer but larger pores on the depolarized hemisphere. At this point, it is worth noting that Deng and co-workers[91] considered a different form of the free energy of the cell membrane by introducing a supplementary strain energy term $U_s(r)$ due to the large deformation of the membrane during EP,

$U(r, V_m) = -\frac{\pi}{2d_m}(\varepsilon_e - \varepsilon_m)V_m^2 r^2 + 2\pi\gamma r - \pi\Gamma r^2 + U_s(r)$. These authors showed that it is this strain energy term that provides resistance to the pore growth and eventually stabilizes the pore size. Tests performed on chicken red blood cells ($R = 10\,\mu$m and $d_m = 10$ nm) determined EP pore nucleation activation energy of the order of $10\,kT$, an equilibrium size of 3.5 nm, and $V_{EP} = 0.82$ V. Kroeger and co-workers[42] have also investigated a curvature-driven pore dynamics model and showed that the aqueous viscosity of the extracellular medium can impact pore dynamics. Recently, a more complicated pore conductance model[26] has been developed based on a continuum Poisson–Nernst–Planck theory considering a toroidal pore shape, pore selectivity for different ionic species, and the electric double layer at the membrane–extracellular medium interface.

The models presented above allow us to study both temporal and spatial aspects of EP. Analysis based on lumped parameter RC models has also been extensively studied in the literature.[13,27–29,33,41] An illustrating example has been recently reported by Sweeney and co-workers[13] to cope with the molecular transport into a single idealized spherical cell immersed in an aqueous buffer. This model (Fig. 5) includes a cell membrane circuit model (reversible primary process) coupled with a phenomenological dual-porosity model and simple diffusion (irreversible secondary process). During the former, a source current I_s drives an increase of V_m (noted U in Fig. 5), with the formation of pores allowing ions to flow across the membrane. Ionic currents slow the V_m increase until a dynamic equilibrium is reached. In the latter, the transport of solute is considered from a high extracellular concentration into a cell initially containing no solute.

A nonlinear size-dependent equivalent circuit (Fig. 6) model of a single-cell EP was presented by Shagoshtasbi *et al.*[92] Based on the Kirchhoff laws and continuity equations, this method allowed the authors to get the time response of V_m, pore size, and pore number at different stages of permeabilization. This analysis relies on an earlier strain energy model[19] that takes into account the change in membrane strain energy due to pore formation (rather than due to a change in membrane tension). The model was designed under the tacit assumption of a uniformly polarized membrane exposed to a pulse shaped electrical stimulus and includes an assumption of nonlinear elasticity in the membrane. Although the main feature of this model is the coupling of the electrical circuit with the mechanical process of EP, it does have several limitations, e.g., this is partly due to the fact that no direct assessment of V_{EP} can be obtained from this model.

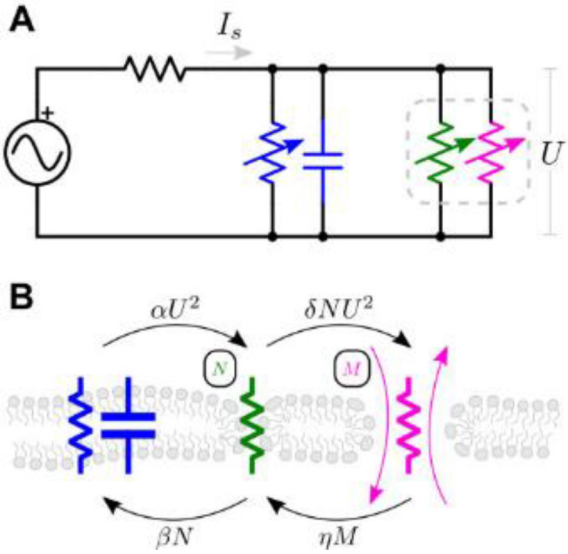

FIG. 5. (a) Electrical circuit model of the cell membrane charging: σ_m is given by the parallel resistance of the naïve membrane (blue, left) and porous membrane weighted by the membrane fraction in each of 2 stages (green and magenta, right), N is the fraction of the membrane area that is conductive of small ions, M is the fraction of the membrane area permissive of the entry of larger solutes, $U = V_m/V_{EP}$, and α, β, δ, and η are constants; (b) The naïve membrane contributes a conductivity and permittivity to the electrical model (blue, left). The N membrane fraction contributes to the permeabilized conductivity of ionic currents but does not permit the transport of larger solutes (green). The M membrane fraction permits diffusive transport of solute (magenta). Reproduced with permission from Sweeney *et al.*, D. C. Sweeney, Technol. Cancer Res. Treatment **17**, 1–13 (2018). Copyright 2018 SAGE Publishing.

F. Multilayer shell models and multicellular system models for understanding tissue-level electric field effects

Evolving subcellular features, e.g., mitochondrial membrane, prominently in models of a biological cell approximated by multilayer spheres with homogeneous, lossy, and dispersive dielectric properties for each layer have been presented (see, e.g., Ref. 48). Multilayered spherical cell models with concentric and non-concentric nucleus were proposed, but considering the full

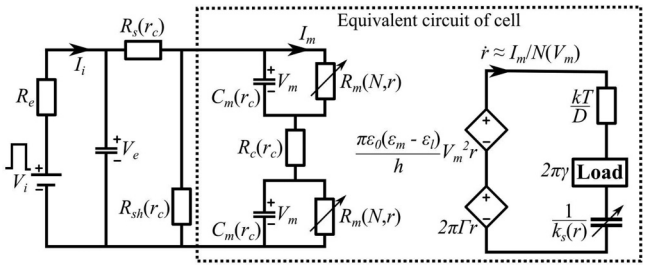

FIG. 6. Equivalent circuit analog describing the nonlinear electromechanical EP model consists of two main electromechanical parts. The dashed line rectangular box includes the components of the cell: C_m, series R_s, shunt R_{sh}, and cytoplasm R_e resistances are functions of the cell size r_c, and R_m is a function of N and r. The equivalent circuit for the pore dynamics is illustrated on the right-hand side. The two controlled voltage sources are the corresponding energy source for the applied voltage and the surface tension $2\pi\Gamma r$. The line tension $2\pi\gamma$ is represented by a constant load; the nonlinear spring $[k_s(r)r]$ for the membrane elasticity is represented by a nonlinear capacitance. The energy dissipative element (kT/D) is represented by a resistance. The total current passing through the cell membrane I_m is part of the total EP current I_i. Reproduced with permission from Shagoshtasbi *et al.*, J. Lab. Automation, 1–10 (2015). Copyright 2015 SAGE Publishing.

morphological information in these models is elusive without precise 3D spatial and dynamical data.

Lumped parameter models can also connect cell-level description to tissue-level phenomena.[93–95] A transport lattice model has been used to analyze multicellular 2D structures with nonlinear active sources of V_{rest}, including simple representations of local and passive membrane EP.[56] Kirchoff's laws provide basic procedures for deriving mathematical models for electrical circuits. Within this approach, a cell assembly can be described by a large electrical system in which local RC components interact through paths that connect nearby cells. But overall, these equivalent circuit models of EP are either too complicated (i.e., for very large electrical circuits) or too simplified (i.e., capacitively coupled nearby cells and more distant layers of cells) to be generalizable to realistic tissue models.

G. Benefit of multiphysics simulations

In light of the above debates, a line of works[6,7,9,22–24,103] constructed and studied numerical generic cell-based models for a scan of parameters and cell assemblies by making use of multiphysics simulations. These examples are not meant to be exhaustive, but may indicate how any continuum CS modeling of cells might be approached. Before embarking on a discussion of case studies, it is worth discussing briefly how multiphysics-based multiscale models capture the unique behavior of biological materials. Finding analytic procedures to calculate the electromechanical properties for cells of irregular shape and/or having many neighbors exactly, or even just with high numerical precision, remains generally unsolved. It is important to understand what it means to model cells and tissues, how these models involve scale and complexity at different levels, and what they can and cannot do. Computational modeling possesses several important virtues. Ease of visualization for cell configurations is certainly one. Another is that these techniques connect dynamics on a hierarchy of length and timescales. From a numerical modeling perspective, a physically complete description of the electromechanical properties at very different length scales (membrane thickness, cell size, and customized tissue scaffold) is enormously challenging since it leads to a rapid increase in the computational cost with the system size. Here, the goal is to make things as simple as possible, but no simpler. An added benefit of using numerical techniques is the possibility of tuning ED and EP parameters to experimental data, such as MC and MR and pore density, which are crucial for the accurate prediction of the electrical and mechanical properties.

III. CASE STUDIES AND DISCUSSIONS

In the below cases, we address four subjects. First, the ability for the electric field to instigate cell shape change is probed by estimating the V_m dependence of C_m and R_m of an initially spherical cell under steady-state electric field excitation. We discuss the effects of different material parameters (both under electric field stimulation and deformation conditions) on C_m and R_m. Second, we focus on the old question of membrane electromechanics, i.e., the relationship between forces and electric field. The quantitative determination of the location and magnitude of the effective strain is an important challenge, because it eventually impacts the ED and EP behaviors. These computer simulations should be placed in parallel with the development of experimental techniques that combine optical tweezers (providing measurement of forces at the pN scale) with patch-clamp apparatus (allowing control of the cell transmembrane potential) to investigate the electromechanical properties of cellular plasma membranes.[96] Third, we report on a method for constructing realistic models of tissues based on irregularly shaped cells allowing us to deal with the specific symmetries (e.g., heterogeneity, anisotropy) of their cellular environment, which differ in many ways with the case of a single cell exposed to an electric field. The pressing challenges of a fully reconstructed biological tissue, e.g.,[6] have prevented previous authors from fully working through all the elements of the analysis. The mechanisms behind all of these biophysical effects are active areas of investigation. To demonstrate the applicability of the proposed method, we present a 3D microscopy-based realistic cell model that is able to reproduce the observed ITV cues. Fourth, we perform mutual capacitance calculation between cells in close proximity and highlight its most relevant implications. Appendix A lists the material parameters used in the numerical models.

A. Numerical determination of $C_m(V_m)$ and $R_m(V_m)$ and electrostatic control for an isolated cell model

Since V_m is a crucial parameter for ED and EP because it drives the creation and evolution of pores on the membrane, it is also desirable to examine the dependence of MC and MR as a function of V_m for nonporated membranes. From Sec. II E, the key point to take away for the MC behavior of a single polarized cell model is its quadratic dependence as a function of V_m. For this work, we consider a single initially spherical cell that is modeled as an elastic shell (Young's modulus Y_m) surrounding a homogeneous core cell interior that is elastic. Because the Poisson ratio of soft materials typically ranges within 0.3–0.5, the maximum error in the definition of the elastic modulus due to the unknown Poisson ratio is expected to be <10%. Therefore, it makes sense to characterize the mechanics of cells with just one parameter, the elastic modulus.[36] We also assume that the ED of the cell does not degrade the mechanical properties of the membrane. Physically reasonable parameter selection describing the mechanical and electrical properties of the cell is used.[23] Further technical details, corresponding to our simulation approach, are presented in the supplementary material of Ref. 23.

For our uniform steady-state electric excitation analysis, we study how a cell, initially having a spherical CS structure, responds to the application of a constant applied electric field. In Fig. 7, we plot the MC and MR against the ITV. The results show an increasing trend of C_m and $1/R_m$ with an increase of V_m in the V_m range investigated from 10 mV to 1.4 V. We confirmed numerically the quadratic dependence of C_m, $C_m = C_{m0}(1 + \chi V_m^2)$, where the adjustable parameter has been determined, i.e., χ is in the range of 5.3–8.2 $10^{-2}\,V^{-2}$, and can be understood from the perspective of EL which is the dominant effect for explaining the shape change of the cell if V_m is not too large.[23]

Overall, this quadratic dependence fits with the observed data, but we find that C_m increases more rapidly at larger field strengths, i.e., $V_m > 1$ V.[97] Upon approaching this limit, we observe a significant deviation from prolate cell morphologies as illustrated in Fig. 7.

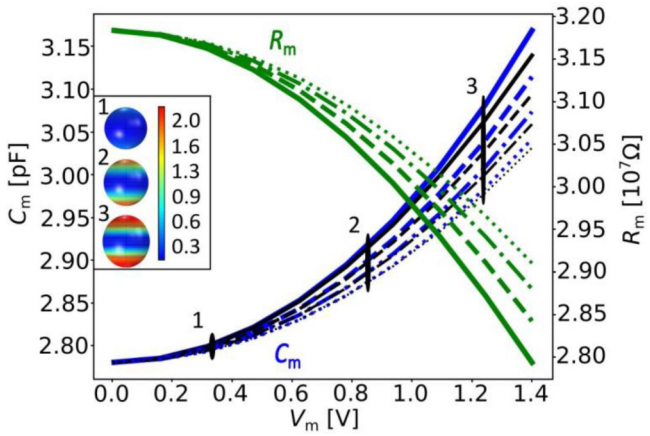

FIG. 7. Evolution of MC (blue lines) and MR (green lines) as a function of the ITV for an isolated cell model.[23] The corresponding numerical values are d_m = 5 nm, R = 5 μm, $\sigma_m = 5 \times 10^{-7}$ Sm^{-1}, $\epsilon_0\epsilon_m = 4.4 \times 10^{-11}$ Fm^{-1}, σ_c = 0.2 Sm^{-1}, $\epsilon_0\epsilon_c = 7 \times 10^{-10}$ Fm^{-1}, σ_e = 0.2 Sm^{-1}, $\epsilon_0\epsilon_e = 7 \times 10^{-10}$ Fm^{-1}, Y_c = 1 kPa, and $V_{rest} = -0.07$ V. In these numerical simulation data, the membrane Young modulus Y_m is varied from 19 MPa (solid line) to 22 MPa (dashed line) to 25 MPa (dashed dotted line) to 28 MPa (dotted line). The quadratic fits of MC are shown in black. The inset illustrates the deformed 3D steady-state geometries of the cell for three different values of V_m. The color bar represents the electromechanical force (units: 10^7 N/m^2) acting on the membrane, and points A, B, and C correspond to the aspect ratios of 1.004 at 19 MPa (1.002 at 28 MPa), 1.03 at 19 MPa (1.02 at 28 MPa), and 1.07 at 19 MPa (1.04 at 28 MPa).

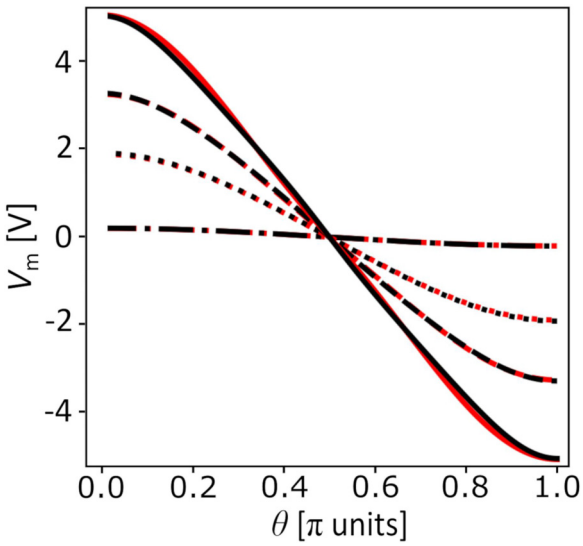

FIG. 8. A comparison of the ITV from our numerical simulations (red lines) with the analytical formula of $V_{m,analytical}$[4] (black lines) at similar aspect ratios for an isolated cell model: a and b characterize the spheroidal cell, being the long and short semi-axes, respectively, and θ denotes the angle between the surface normal and the field direction. Y_m = 19 MPa, and we keep all other structural and material parameters similar to those used for obtaining Fig. 7. We show the evolution of different choices of the steady-state electric field value, which is increased from 0.3 kV/cm (dashed dotted line) to 2.4 kV/cm (dotted line) to 3.7 (dashed line) to 5 kV/cm (solid line) for which the corresponding aspect ratio values are 1.02, 1.08, 1.19, and 1.36.

Consequently, the cell shape is no longer spheroidal. A close inspection of the aspect ratio change follows the C_m behavior up to $b/a \cong 1.4$ (Fig. 7), beyond which the large strain produces complex axisymmetric cell shapes that can be described using a variety of different parameterized forms, e.g., Cassini curves.[98] This shows an important finding that the higher the ratio, the more dominant the effect of the TMP which increases the MC and decreases the MR. Another fact arising from our simulation is that $R_m(V_m)$ does not scale as V_m^{-1}, as suggested by Morshed and co-workers,[75] but as V_m^{-2}.

With an understanding of the ITV sensitive capacitance behavior of a cell membrane under steady-state electric field excitation, we performed additional simulations to investigate the ellipticities and associated 3D cell shapes, and whether they might be prolate or oblate depending on the polarization and magnitude of the electric field excitation.[23] There is no general analytical formula of V_m which can be used for arbitrary cell shape, but analytic calculations allow one to compute V_m; see, e.g., Ref. 4, for a prolate spheroid with the axis of rotational symmetry aligned with the electric field, $V_{m,analytical} = E\frac{(b^2-a^2)}{b-\frac{a^2}{\sqrt{b^2-a^2}}\log\left(\frac{b+\sqrt{b^2-a^2}}{a}\right)} \times \frac{a\cos(\theta)}{\sqrt{b^2\sin^2(\theta)+a^2\cos^2(\theta)}}$.

Using the procedure outlined above, we performed a set of calculations for different values of the steady-state electric field ranging from 1 kV/cm to 5 kV/cm, i.e., different values of the aspect ratio b/a ranging from 1.02 to 1.36. We find that $V_{m,analytical}$ reproduces the numerical results to better than 5% accuracy over the range of θ explored (Fig. 8).

Notice that in the numerical approach taken here and for our choice of parameters, we find that the membrane thickness is not uniform. Consequently, significant deformations of the membrane can arise (up to 5%). We will quantify the differences in d_m by calculating $\delta d_m/d_{m0}$ which decreases approximately quadratically with electric field strength, where d_m is the effective membrane thickness under electric field excitation and d_{m0} is the unperturbed membrane thickness. We also compare our data to $d_m = d_{m0} - c\cos^2(\theta) + d\sin^2(\theta)$, where c and d are two constants.[23] The fit obtained this way is plotted as a solid line in Fig. 2(b) of.[23] Positive values of $\delta d_m/d_{m0}$ denote tensile strain, whereas negative values denote compressive strain.[23] A 500-mV increase causes a 1.5% increase in C_m, 0.7% d_m decrease, and 0.7% A_m increase such that the nominal volume of the membrane remains constant. This is corroborated by experimental data showing that the thickness of the membrane does not change by more than a few percent throughout the EP process.[82]

While these preliminary simulations present an opportunity to witness complex dielectric phenomena in cell membranes, they suffer from a number of limitations. First, our analysis has focused on nonporated membranes. In Ref. 14, Weaver and co-workers estimated the contribution of transient aqueous pores to capacitance and found that the time average property of a large population of transient aqueous pores has similar features with a quadratic dependence of capacitance. Second, an important constraint of the

continuum model comes from the fact that the MC and MR features are independent of the molecular details of the membrane in which they occur but are dominated by the geometry and can be explained with simple mechanical models. Schwan's equation predicts that cells should porate at threshold electric fields that go as R^{-1}; however, the authors of Ref. 99 found that the electric field needed to induce poration that varied between three types of cells, but all of them confirmed the lack of size dependence. It is also worth referring to a recent study of Liang and co-workers.[100] In this study, the authors reported on a 3D analysis of the positive and negative optically induced dielectrophoresis (ODEP) forces on cells stimulated by a nonuniform ac bias potential. The MC per unit area and areal MR of four types of cells were derived by characterizing their ODEP crossover frequencies using micro-vision techniques and were found to be of the order of $10^{-2}\,\mathrm{Fm}^{-2}$ and $10^{-2}\,\Omega\,\mathrm{m}^2$, respectively, i.e., remarkably close to the estimates found in Sec. II B and to our numerical data. Third, we made the assumption about the scalar nature of the membrane permittivity. It can be argued that this assumption is not very physical (i.e., the cell membrane is heterogeneous and the electric-field induced stretching of the membrane exhibits a peculiar anisotropy), but nevertheless our results allow us to shed some light on the mechanical strain involved in the ED. Fourth, in Ref. 23, we provide another figure when the conductivity ratio between the cytoplasm and the extracellular medium varies by two orders of magnitude but keep all other structural and material parameters constant. We find that C_m and R_m are weakly affected only in the range of the electric field magnitude explored. We further note that the charge near the membranes (ionic double-layer) contributes with a capacitance that acts in series with C_m. Within a mean field approximation,[8,] i.e., assuming that the double layer capacitance is equal to the capacitance of a planar capacitor with thickness equal to the Debye length and permittivity $\epsilon_0\epsilon_\mathrm{e}$, a correction to the C_m value is obtained at the percent level in accordance with experimental capacitance values for biomimetic bilayer membranes at different solution conductivities.[77] Fifth, since we considered only a single cell, a statistical analysis that considers the influence of different variables was not possible. These trends, we believe, are real despite the limitations. Also, note that this model is flexible to incorporate a variety of other biological attributes such as internal organelles and nucleus membrane. Here, the cell membrane is assumed to have elastic properties when stretched. An obvious next step is to consider viscoelastic (or even poroelastic[21]) cell materials; however, this is a much more difficult problem, because the mechanism by which the membrane is deformed is crucially affected by the detailed temporal sequence of electric field excitation.

B. Strain energy in multicellular environments and membrane electromechanics

Thus far, we have presented evidence that our numerical simulations exhibit elastic membrane deformation consistent with a prolate cell morphology. Another kind of question that is of interest from a quantitative modeling perspective includes the description of strain energy in cell assemblies.[22] These discrete cell models are useful to predict the behavior of an individual when mechanical properties are changed either intrinsically or driven by an electric field excitation. First, we use FE in the framework of a time domain to solve for the ED and cell EP when a well-defined electrical stimulus is delivered to a multicellular environment. There is increasing interest in using high-frequency electric fields to manipulate cells and tissues. Second, the strain–stress response of the cell assemblies is characterized by a relaxation time that is much larger than the time constant of the membrane charging. We begin by summarizing the formalism presented in Ref. 22. The individual cells are not in contact with each other. The CS cell models are 3D, and intercellular distances range from $0.625\,\mu$m to $5\,\mu$m with a thin membrane (set to 5 nm) maintaining the cell integrity and selective transport of substances in the cell. The interior of the cell (cytoplasm) is assumed to be homogeneous. The individual membrane is modeled as a viscoelastic structure surrounding an elastic cell interior. Each cell is initially a sphere, and the cell shape and size vary as the electric field excitation deforms it axially. In terms of earlier notation, a small-scale phenomenology allows to obtain the surface electric field from the solution of electric potentials that are coupled at the cell membrane through the specific boundary condition given by $\boldsymbol{n}.\boldsymbol{J} = \frac{1}{d_m}(\sigma_m + \varepsilon_m)\partial t\ (V_{int} - V_{ext})$, where $\boldsymbol{n}$ is the unit vector normal to the boundary surface, $\boldsymbol{J}$ is the electric current density, ∂_t denotes the time derivative, and "int" and "ext" denote the cell interior and exterior sides, respectively. A resting potential of −50 mV is set and the conductivity and permittivity values for the interior and exterior side of the cell and for the membrane have standard values.[3,27] The resulting stress distribution is coupled to the structural model for calculation of membrane displacement u. In the case at hand, the strain energy was calculated by solving first $\rho\partial_{t^2}^2 u = \nabla.S$, where it should be borne in mind that ρ denotes the mass density and S denotes the stress.[20] The strain energy of the cell membrane can be calculated for both deformable materials as $E = \iint S\gamma\ \mathrm{d}\Omega/2$, where γ is the strain and $\mathrm{d}\Omega$ is the volume or surface element. Standard parameter values describing the cell mechanical and electrical properties are used.[22] Technically, we give the concrete details of the FE simulations in the supplementary material of Ref. 22. This case study is interesting because it considers the thin membrane thickness with an analysis in which the membrane is modeled as a distributed impedance boundary condition.

We impose various pulsed field pulses[22] and analyze the pore dynamics during pulsing. For simplicity, all pores have the same size (0.75 nm), which does not change with time. The pore density in the membrane is calculated with the Neu and Krassowska model on the basis of the highly nonlinear dependence on ITV, i.e., which alters the initial cell membrane conductivity by adding the following term $\sigma_{EP} = N(2\pi r_p^2\sigma_p d_m/(\pi r_p + 2d_m))$, where we denote the density of pores in the membrane, the radius and the internal electrical conductivity of a single pore, and the membrane thickness by N, r_p, σ_p, and d_m, respectively.[54] Then, the number of pores involves surface integration of pore density over the total cell membrane surface area, so we obtain $N_{pores} = \iint N dA$.

We rationally designed eight examples of seven CS arbitrary fixed in space cell configuration (Fig. 9) which are subjected to an electric field pulse excitation and tested them for evaluating the time evolution of strain energy and membrane displacement. The electrical excitation is a positive polarity trapezoidal voltage pulse (applied in the z direction) which delivers an average electric field of strength $E_0 = 5$ kV/cm.

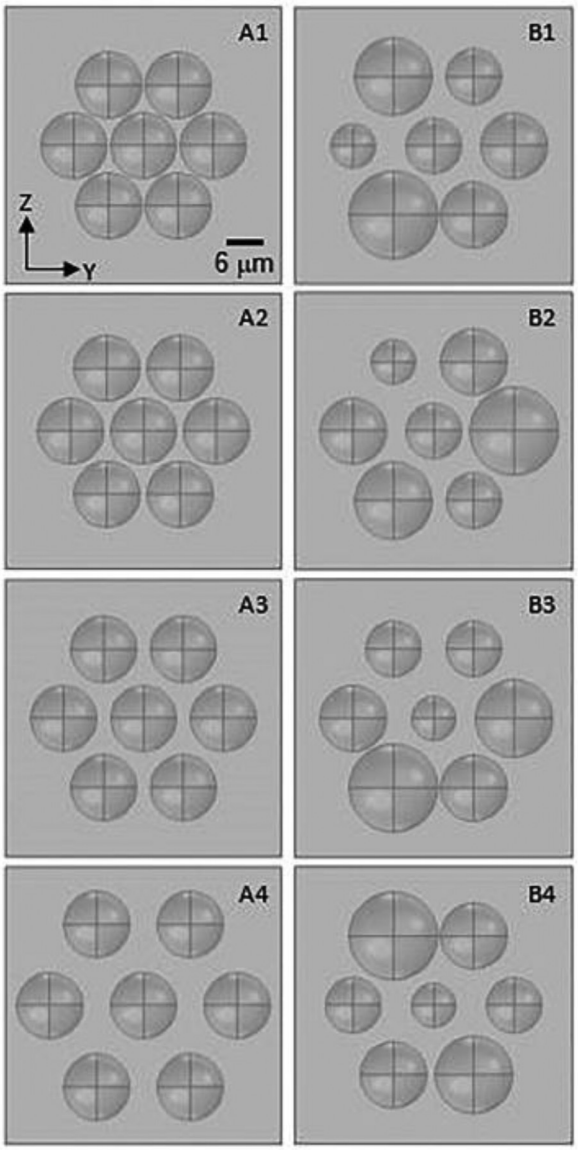

FIG. 9. Schematic of the eight canonical examples of a seven-core-shell arbitrarily fixed in space cell configurations and subjected to an electric field pulse. In the A1–A4 configurations, all cells have the same radius set to 6 μm, and the intercellular boundary–boundary distance, $d_{b\text{-}b}$, with respect to the central cell is varied from 0.625 μm (A1), 1.25 μm (A2), and 2.5 μm (A3) to 5 μm (A4). In the B1–B4 configurations, cells have a radius distribution leading to a broader $d_{b\text{-}b}$ distribution with a minimum set to 0.5 μm with respect to the nearest neighbor. The side of the computational cube domain is 50 μm. Reproduced with permission from D. Shamoon, S. Lasquellec, and C. Brosseau, Appl. Phys. Lett. **115**, 043701 (2019). Copyright 2019 AIP Publishing LLC.

Shamoon and co-workers[22] analyze their data to calculate, among other things, the strain energy for the viscoelastic membrane as it determines its ability to sustain its shape under electrical stress. Under Maxwell stresses, initially spherical cells deform into prolates, with the longer axis oriented along the electric field direction. Furthermore, they reported a "switch off" phenomenon for several kinds of electrical stimuli observed in different cell configurations and a detailed study of the parameters affecting the temporal dynamics of the local enhancement of the electric field, the surface charge density, the polarization distribution, the relative deformation, the elastic strain energy, and the pore area extent within the cell membrane. The effects of symmetry and proximity on the elastic strain energy distribution of the viscoelastic membrane for the different configurations are shown in Fig. 10. First, there is a general pattern in these graphs in the "switch on" state, i.e., a narrow peak during a few tenths of μs followed by a broad plateau. Second, it is noticeable that in the "switch off" state, a second peak is observed with a timescale that can range from several tenths of μs to 200 μs. The "off" state reflects the dominance

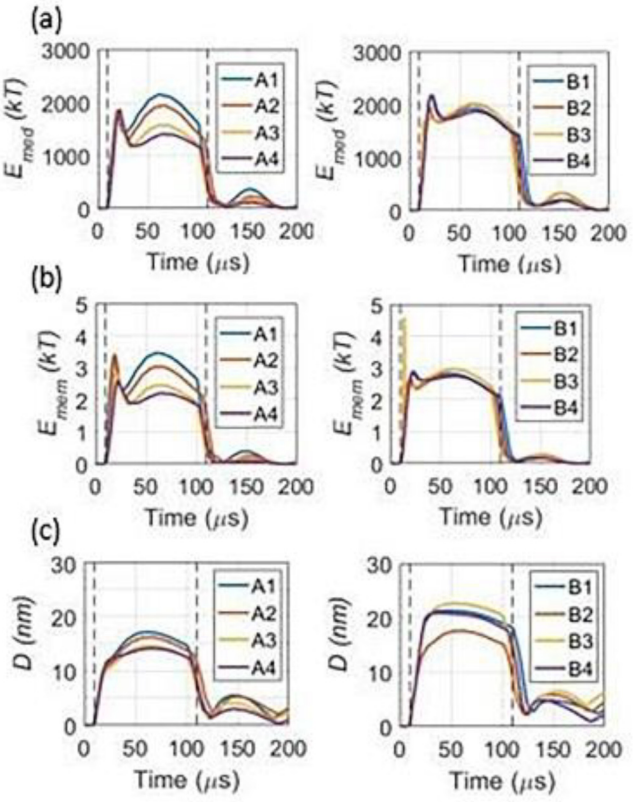

FIG. 10. Time evolution of the strain energy in seven-cell configurations vs time when the different configurations are excited by pulse, which begins at 10 μs and ends at 110 μs. The limits of the pulse are marked with vertical dashed lines. The dashed lines indicate the beginning and end of the pulse. (a) Strain energy for the interior and exterior of the cell, (b) strain energy for the viscoelastic membrane, and (c) the maximum value of the membrane displacement for the different configurations studied. Physiological conditions (T = 310 K). Reproduced with permission from D. Shamoon, S. Lasquellec, and C. Brosseau, Appl. Phys. Lett. **115**, 043701 (2019). Copyright 2019 AIP Publishing LLC.

of the mechanical relaxation process over the electrical charge relaxation. The "switch off" signal is likely observable in currently AFM-based, scanning probe and confocal fluorescence microscopy experiments under *in-vivo* experiments and could be used to probe cellular tensegrity in tissues and other biological structures at smaller and larger size scales. This model can produce large linear strain energies for the membrane of a few kT in magnitude and extremely high displacements of over 300% in magnitude (Fig. 10).

There is scope to improve this kind of computational approach by introducing cell structural complexity compared with this simplistic mechanical model since recent research has shown that cells are able to sense mechanical signals and forces in their environment. In pursuit of this, these results indicate a possible correlation of elastic strain energy and membrane displacement. The ability to inhibit and/or control the "off" state is important for applications in the field of ultrasensitive clinical diagnostics, tissue engineering, and biologically inspired materials for tissue repair and reconstruction. Furthermore, the impact of each parameter of the Neu and Krassowska model is highly non-uniform due to the nonlinear parametrization. As briefly covered above, there is a lack of experimental data to characterize the mechanical properties of electroporated cells and tissues to confront with numerical predictions. So, from both a fundamental perspective, i.e., how the mechanical signals are converted into an intracellular biochemical response, and an application perspective, these results have significance, because they can open newer doors to be used for 3D engineered tissues.

C. Multicellular environments and tissue EP

Another central theme of this tutorial is the development of 3D microscopy-based realistic cell models for tissue EP from a coarse-grained (continuum) perspective.[6] Several strategies can be employed to analyze the EP in tissuelike structures, i.e., shape adapting to the environment without compromising functionality. Many analytical formulas for the cell shape were generated for a specific structure, but there is no general form that can be used for all materials.[98,104,105] Progress has been also reported in predicting cell shape by analyzing their contours, e.g., phase-field[104] and Potts models.[105] These works have enhanced our understanding of the dynamics of non-axisymmetric cell shape and ED forces when cells are exposed to pulse electric fields.

In Ref. 6, in an attempt to replicate realistic cell shapes, a general procedure is proposed to generate simple cell shapes in 2D, which uses the reconstruction of biological structures based on microscopy characterization and is applicable to a variety of cells. This scenario exploits fluorescence microscopy bitmap images [Fig. 11(a)] to generate the piecewise continuous mesh used to develop a 2D FE element model [Figs. 11(b) and 11(c)]. Then, each cell is narrowly confined by the presence of its immediate neighbors that themselves are narrowly confined. This provides a means to determine the ITV for cells of irregular shape and/or having many neighbors, since V_m cannot be derived analytically. To illustrate the potential power of this technique, a 2D implementation is illustrated below. Such a method has been demonstrated to produce experimentally consistent dense disordered multicellular environments whose electrical properties can be analyzed. These results

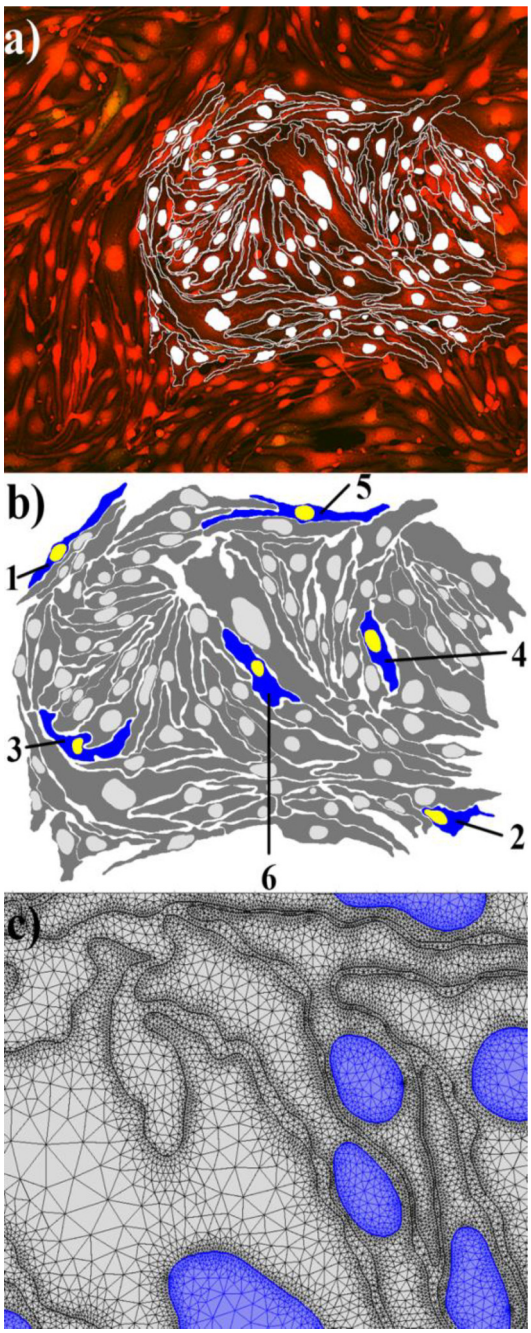

FIG. 11. Steps taken when transforming a microscopy bitmap image to a COMSOL® geometry. (a) Fluorescent microscopy bitmap image with traced cell edges and traced nuclei edges, which were also colored in white. (b) Final bitmap image of the cells and their nuclei, used to create the geometry used in the COMSOL® model. The numbers 1–6 denote the cells used in a separate model.[6] (c) Zoom of a part of the entire geometries used in the COMSOL® model, illustrating the dense edge (cell and nucleus membrane) meshing. The blue color represents the nuclei [Reproduced with permission from Murovec *et al.*, Biophys. J. **111**, 2286–2295 (2016). Copyright 2016 Elsevier Publishing].

can be leveraged to 3D geometries using a similar protocol and confocal microscopy images.

Following the method described in Ref. 6 to obtain the pre-EP ITV induced in tightly packed cells (the six-cell configuration shown in Fig. 11), the next figure, Fig. 12, examines the ITV along a reference cell membrane [cell 4 in Fig. 11(b)]. Of course, the dense packing of cells disrupted the uniform electric field gradient that is observed when the six cells are isolated. In the case of an isolated cell, it is also interesting to note that the ITV is significantly larger than the packed cell configuration. This decrease of V_m in a densely packed environment is consistent with several experimental studies reported in the literature, e.g., Ref. 101. We also note that Schwan's equation (Sec. II C) cannot capture most of the features of V_m shown in Fig. 12 for an equivalent cell radius, i.e., a circle with an identical area of the cell. Reference 6 also argues that a significant difference between the densely packed layer of cells and the isolated scenario is observed in which the ITV is significantly larger when the cells are isolated. Currently, this model is limited in scope by the data with which it has been checked and validated. This model offers a viable perspective to the challenge of consistently generating a numerical model of many cell configurations. In principle, this approach can provide generalization when a variable membrane conductivity dependent upon the induced ITV can effectively model pore formation.

D. Proximity-induced ED and capacitance coupling between cells

The fundamental physical resource for performing various biochemical processing tasks is the interaction between cells. In the interest of promoting broader discussion about collective effects in cell assemblies, it seems appropriate to describe mutual capacitance arising from short-range interactions between cells. This is an important issue since cells in multicellular organisms sense their location within tissues via diffusible molecules, contact interactions, and mechanical signals.[102] In tissues, cells form electrical connections with their neighbors via gap junction channels. One can then ask whether this capacitance coupling (CC) is a minor perturbation on the individual cells or whether it plays an important role in the dynamics of bioelectric cues.

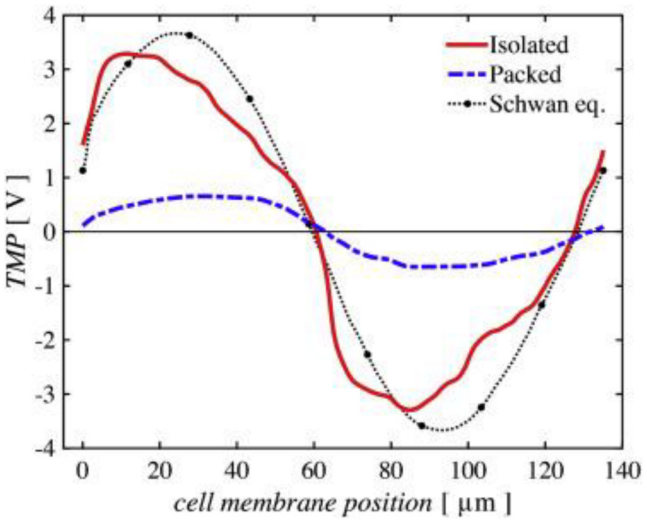

FIG. 12. ITV variation along the membrane of a reference cell [Fig. 11(b), cell 4] when it is isolated (red solid line) and surrounded by other cells (blue dashed line) during the pulse (20 μs) excitation,[6] compared with the analytical calculation based on Schwan's equation with constant radius (dotted black line, circle marker). Reproduced with permission from Murovec *et al.*, Biophys. J. **111**, 2286–2295 (2016). Copyright 2016 Elsevier Publishing.

Progress in understanding, predicting, and controlling CC has been, on the whole, limited by the lack of two factors: first, from a theoretical perspective, currently there exists no general framework to quantify CC in the literature; and second, techniques to generate reproducible and accurate MC measurements are very challenging. As articulated in Sec. III A, the change in C_m is directly related to the change in membrane thickness. The results presented herein are acquired through the use of methodology presented in the supplementary material of Ref. 106. Here, we concentrate on surmounting the significant technical issues of systematically studying the ED and CC between a pair of cells arising so as to better quantify the complexity inherent in tissues. Addressing this source of complexity will eventually require research-area-specific experimental and theoretical advances, but the growth in computational power also opens up the possibility of outsourcing some of the analytical burden to high-throughput computing resources.

We show that an emergent behavior arises by considering the separation distance-orientation angle diagram when the difference between the ED force for a pair of cells and its counterpart for a single reference cell is analyzed. This allows a consistent analysis of the CC anisotropy. Here, r is the distance between the two cells and θ is the orientation angle relative to the electric field direction. The case of steady-state electric field excitation is first considered with magnitude $E = 1.9$ kV/cm. It should be noted that the corresponding maximum value of the ITV at the cell's poles is 1.4 V, which is less than the maximal value of the membrane EP voltage threshold, i.e., 1.5 V.[4] For a frequency-dependent field excitation, the model is valid within the quasistatic approximation. The cell is described as an elastic membrane surrounding an isotropic and homogeneous cytoplasm that is elastic. The membrane and the cytoplasm are purely elastic materials, with their respective Young's moduli set to $Y_m = 19$ MPa and $Y_c = 1$ kPa.

The key point to take away is that beyond a threshold separation distance, the excess ED force becomes independent of the separation distance and the cell pair becomes non-interacting (gray region in Fig. 13). At the same time, it is informative to observe the flatness of V_m and $\delta_m = d_{m0} - d_m$ (what exactly is meant by these parameters is discussed in the supplemental material of Ref. 106) which parameterizes the field-induced change in membrane thickness which generally varies with position over a cell membrane. For illustrative purposes, we indicate the membrane capacitance per unit area of the reference cell for three points, A, B, and C, corresponding to different regions of parameter space in the r-θ plane: 0.0099 F/m^2, 0.0097 F/m^2, and 0.0108 F/m^2, respectively. For A, we find that the membrane capacitance per unit area reproduces well the value found in Refs. 23 and 106. We further note that we have a 11% increase in C_m between the two specific points B and C ($r = 1.05\,\mu$m) that can be accounted

for by a significant CC coupling between the two cells in the amplification region of the distance-orientation angle diagram. One can also see from the figure that there exists an angle θ_c for which the excess ED force vanishes.

To further investigate the different regions in the r-θ plane, we dissect the individual effects of the geometrical property of extracellular space (conductivity ratio $\Lambda = \sigma_c/\sigma_e$ between the conductivity of the cytoplasm σ_c and that of the extracellular medium σ_e) and with frequency of the excitation field by changing only one parameter at a time and keeping all other parameters constant. Our discussion is now framed around the ED response with frequency of the excitation field. We consider two different values of the frequency of the applied field ranging from 50 Hz [below the α-dispersion (1 kHz)[2,3]] to 50 kHz. The different panels in Fig. 14 show several important findings.

By comparing with Fig. 13, we observe that the shape of this diagram, as σ_e is increased from $0.05\sigma_c$ to $20\sigma_c$ ($\sigma_c = 0.2$ S m^{-1}), remains very similar to that shown in Fig. 13 below the α-dispersion. However, when the α-dispersion frequency is crossed, the θ-dependence of the excess ED force attenuation–amplification transition exhibits an inversion compared with Fig. 13, and the position of θ_c varies with Λ as shown by the crossover lines of the transition depicted in (Fig. 4 of Ref. 106). Additionally, this spectral property makes our analysis a very interesting object for more formal and experimental applications as it allows a physical interpretation in the context of the attraction–repulsion transition of electrostatic forces between biological cells.[103]

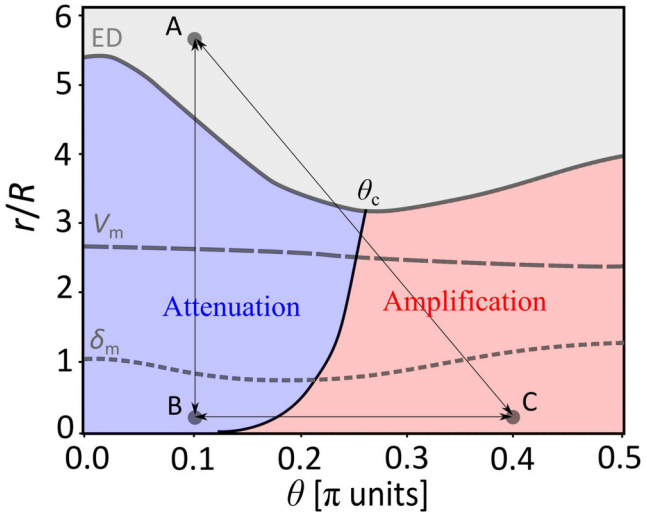

FIG. 13. Regions in the separation distance-orientation angle diagram for the excess ED force. The gray region indicates the region in the r-θ plane for which the absolute value of the excess ED force is less than 5%. The line corresponding to the null excess ED force is described by angle θ_c. Additionally, this diagram illustrates the distance-orientation range for which the absolute deviations of V_m (dashed line) and δ_m (dotted line) are less than 5% (see Ref. 106 for definitions). Three particular points of this diagram are considered for discussion of the CC: A ($r = 28.6\,\mu$m, $\theta = \pi/10$), B ($r = 1.05\,\mu$m, $\theta = \pi/10$), and C ($r = 1.05\,\mu$m, $\theta = 4\pi/10$).[106]

Together, these results demonstrate that ED and C_m are sensitive to the proximity of neighboring cells, which eventually induce anisotropic perturbation of the local electric field distribution in a cell assembly and/or a tissue. While there are no directly comparable experiments, these results can be qualitatively compared to a variety of observations published in the archival literature.[22,96,107,108] One of the mutual capacitance "issues" that deserves some thought and discussion is the connection between the broad modeling opportunities offered by computational simulation techniques on the one hand and the severe constraints on these opportunities required by physical realism to construct cell assemblies and tissues, such as those described in Sec. III C.

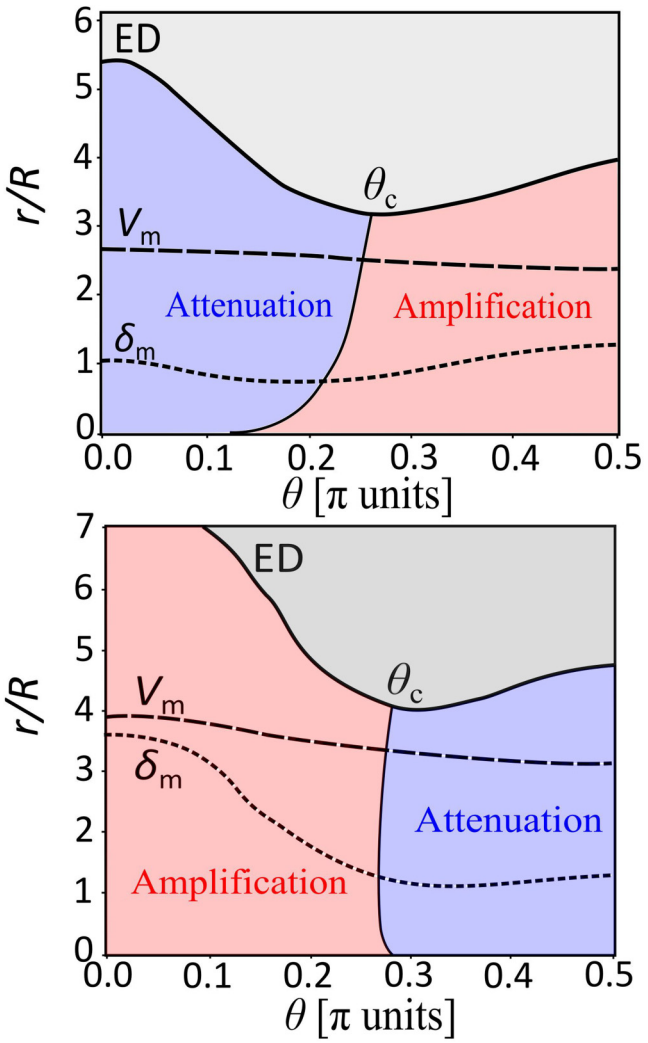

FIG. 14. Evolution of the attenuation–amplification transition of ED force for an ac electric field excitation and different values of the conductivity of the extracellular medium. Top panel: 50 Hz, bottom panel 50 kHz. $\Lambda = 20$, and $E = 1$ kV/cm.[106]

E. Limitations of continuum models of EP

We have sketched just a few examples of how FE simulations will advance our understanding of the ED and electroporation EP biophysical processes occurring in the cell membrane, beyond what is achievable from analytical models. In reaching the end of this section, it is worth emphasizing a list of open questions that FE simulations cannot help us answer, because they disregard the molecular-level structure. First, as a non-equilibrium process on a molecular scale, the EP mechanism is determined by the movement of phospholipid molecules, water molecules, and ions. Continuum models cannot describe molecular scale microscopic processes, such as the molecular and small ions transport across the pores in membrane. Since EP involves a broad range of length scales [from nm (membrane thickness) through μm (cell size) up to cm (tissue sample)] and timescales (from ns to h), understanding its first-principles features requires a multiscale modeling approach, ranging from molecular simulations to large-scale continuum models of cells and tissues. Insights from molecular-level modeling, particularly MD simulations that enhance an understanding of pore formation, and evidence of chemical modifications of membrane lipids have been addressed in the literature; see, e.g., Refs. 12, 26, 45, and 46. Second, FE analysis is useless to analyze the molecular scale configurational states of lipid membranes during pore formation, while MD simulations can provide biomolecular mechanistic perspectives through which many mechanosensitive cellular processes can be quantitatively characterized.

IV. EPILOGUE AND PATHS FORWARD

Early work focused on analytical models that can capture the key features of multiscale processes that occur when cells are electrically stimulated or mechanically stressed. Our theoretical approach was guided by the aim to make the simplest possible models that captured key aspects of cell membrane electrical characteristics. A basic message of this tutorial is that these biophysically inspired electric circuit equivalent models for modeling electrically stimulated deformable membranes are useful, because they rely on few parameters to describe the main features of experiments. Unfortunately, they are available only for a few biological materials and cell configurations. To compete with more general first-principles methods, the research community is just beginning to explore computational models that can be developed for any material and cell assemblies.

A. Summary

We conclude by reiterating a few important points of this multifaceted Tutorial. A comprehensive description of deterministic RC approaches based on continuum theories is first provided. These calculations and experiments show the relative importance of the membrane compression vs V_m. At low values of V_m, MC varies quadratically as a function of V_m and MR is infinite, but as V_m is increased at a value below the EP threshold, the membrane should be considered as a nonlinear capacitor. Over the EP threshold, V_m and MR decrease due to the charge transport across the membrane. On the other hand, stochastic mechanisms of pore creation, destruction, and evolution included in several transient aqueous pore models of EP based on Smoluchowski are described. These models differ in the formulation of the expression of the pore creation energy and the description of the resistance of an individual pore. However, the validity of the Smoluchowski equation has been questioned for submicrosecond pulses for which the timescale to form a hydrophilic pore may be longer than the time that large V_m exists.

On the simulation side, continuum and deterministic FE analysis has proven to be a powerful technique to deal with the complexity of the ED and EP of outer cell membrane mechanisms. These model building approaches are able to predict both spatial and temporal resolutions of the electric field and strain distribution in the cell and can serve as a benchmark for quantitative comparison with methods based on lumped electric circuit equivalent models and experimental observations. To summarize our findings concerning the electromechanical properties of strained biological cells, we show that a quadratic dependence of membrane capacitance and conductance captures the impact of the strain state of an isolated cell model under electric field excitation. An added benefit of using FE analysis is the possibility of tuning electromechanical parameters to experimental data, such as ED, V_m, and CC, which are crucial for the accurate description of bioelectric cues. Using a theory-based cell system model, we examine how an ensemble of cells responds to the application of a constant and uniformly applied electric field. These numerical models highlight the significant differences between isolated and tightly packed cells. This paper also reveals the existence of a critical separation distance-orientation angle diagram providing evidence of a separation distance beyond which the electrostatic interactions between a pair of biological cells become inconsequential for the ED. There is now a widespread recognition that tissue engineering requires a firm understanding of the underlying CC that occurs within the cell assemblies under consideration. Our findings underscore the structural parameters (cell aspect ratio, membrane thickness, and surface area) as efficient tools to tailor the effective electromechanical properties of membranes that affect proximity-induced CC between cells. This introduces the interesting prospect that these phenomena are coupled. Clearly, if one wishes to further exploit the potential of numerical models with realistic cell morphologies for clinical applications, a multiphysics study into the pore formation that occurs during the application of electric pulses is warranted. Of course, no one believes that membrane ED and EP are ever actually this simple. Nevertheless, these idealized models have widespread influence, because there are countless complications that could, in principle, matter, and it is impossible to model all of them at once. We highlighted several case studies as they serve to exemplify two sources of complexity: separately, each case presents an incredibly rich set of questions and problems that are in some cases already pushing the limits of computational capability; in combination, they represent a multi-scale challenge that starts at the molecular scale through the cellular and tissue levels.

B. Several open challenges and opportunities

The challenge of how to build quantitative models of complex systems such as biological tissues with many interacting degrees of freedom is not new, but the use of computer simulations clearly

changes the story. There has been great progress in recent years from a number of different quarters in developing robust numerical simulations for ED and EP modeling, but it seems that every new model presents unforeseen numerical and physical challenges. One key aspect of the continuum description that was not considered in our numerical simulations is the inhomogeneity and anisotropy in material properties of the cell such as conductivity and permittivity. Clearly, more thought should be given to predictive multiscale models in which the microscopic physics is maintained only where needed. Another most promising approach is to include hysteretic behavior of the MR change of an electroporated membrane due to recovery (resealing[68]). Typical elastic and viscoelastic modes would require average properties of several millions of cells on a millimeter scale.[97] Additionally, voltage-gated specific ion channels have the ability to affect membrane barrier permeability and should be inextricably linked to changes in electrical parameters that include local MC and MR, so the state of strain of membrane cells under electrical stimulation should be inferred by sensing these channels.

A vast amount of evidence exists for the presence of nanoscopic pore formation in cell systems under electric field stimulation, but our understanding is incomplete both from theoretical and experimental standpoints. More specifically, a visualization of the presence of electropores is difficult in practice, since their transient nature and small size place strong limitations on the experimental characterization of their detection and growth dynamics. At the time of writing, one of the flagship techniques for examining membrane EP is to use fluorescence imaging generated by the ionic flux, e.g., Ca^{+} and K^{+}, through a pore.[59,68,105] A wide variety of direct and indirect EP detection experiments are actively searching for evidence of pores depending on many physical parameters and environmental factors that can introduce large uncertainties in making theoretical predictions. However, their origin, dynamical formation, and statistical distribution of size remain a crucial open question, especially on scales where we have no direct observations of the detailed inner structure of membranes.

There is an ongoing effort suggesting that ED and EP mechanisms like those described above are governed by an intricate interplay between, for example, electrostatic repulsion and attraction forces, mechanical deformations, thermal energy, and chemical bond energies. These mechanisms involve multiple scales in space (Figs. 8 and 10) and in time (Fig. 1), but also in energy, which reflect the rich interplay between deterministic and stochastic energies that dictate phenomena in nearly all the molecular processes of life. On these scales many fundamental physical concepts have a large impact on biology, among them are thermal fluctuations, cooperativity, self-assembly, or elasticity. We observe that membrane strain energy (~5–10 kT) and whole media strain energy (~10^3 kT) estimates from our numerical models[22] are well within the range of the physically relevant processes displayed in the energy metrics diagram shown in Fig. 15.

Thermal fluctuations agitate molecules in solution over a broad range of times and distances. Since the population of pores in the membrane is attributed to thermal fluctuations, it is also interesting to compare the relevant energies in ED and EP to kT. The scale kT is important since processes that operate on the scale of kT or below happen spontaneously and reversibly.

The field of cell membrane EP and ED is still a little theory and computation heavy, and a direct comparison of numerical

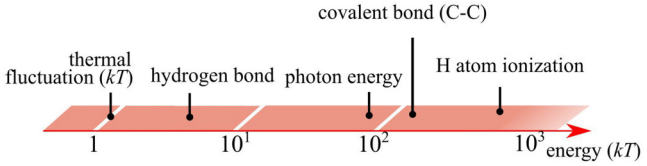

FIG. 15. Illustrating the energy scale (in terms of the thermal energy scale kT) in the cellular context.

simulations to quantitative experimental data is yet to be made. We have yet to fully optimize the modeling analysis of the ED and EP of cell membranes in order to take full account of the cell shape change and spatiotemporal dynamics of EP. As illustrated above, we are also interested in how C_m, R_m, and V_m sense changes in the extracellular environment. From a practical perspective, such models could also help predict the dielectric and mechanical behaviors of healthy and cancerous cells which have been found significantly different from their healthy counterparts, e.g., cancer cells have more negative charges on their surface, a lower V_m, and a lower electrical impedance than normal cells.[110] These approaches can eventually provide us a better physical intuition for the parameter dependence of the dynamics of each individual pore, including location on the membrane, creation, destruction, and size evolution, and thus help us to better understand much complex challenges such as the DNA electrotransfer and endocytosis (i.e., electrointernalization[110]) mechanisms. Very little is known about the spatiotemporal distribution of defects into the membrane, and even less about nanostructured components that might be a small fraction. However, it is precisely these small but interesting components that might prove to be the most spectacular on the voltage-gated ion channels.[111]

While this foreshortened list of several key challenges remaining before the ED and EP of cell membranes can be fully understood, it is useful to keep in mind that this field of research has reached a stage where it captures the imagination, inspiring innovative goals for engineering cellular systems to carry out specific functions. As discussed by Selberg and co-workers,[112] the fields of synthetic biology, which focuses on genetic and cellular substrates, and of bioelectronics, which focuses on interfacing electronics with biology, have made significant advancements that now allow for convergence.

AUTHORS' CONTRIBUTIONS

All authors contributed equally to the work.

ACKNOWLEDGMENTS

E.S. would like to thank Université de Brest for supporting this research through its Ph.D. program. This work was performed under the auspices of Lab-STICC which is Unité Mixte de Recherche CNRS 6285.

Appendix A: Physical parameters used in numerical simulations[6,22,23,106]

The purpose of this appendix is to provide the reader a detailed list (Table II) of the input parameters used in our FE

TABLE II. A summary of the parameters used in the FE analysis of biological cells exposed to electric fields.

Parameters	Notation	6	22	23	106
Cell radius	R (μm)		6	5	5
Membrane thickness	d_m (nm)	5	5	5	5
Cytoplasm, permittivity	$\epsilon_0\epsilon_c$ (F m^{-1})	5.3×10^{-10}	5.3×10^{-10}	7×10^{-10}	7×10^{-10}
Cytoplasm, conductivity	σ_c (S m^{-1})	0.5	0.42	0.2	0.2
Membrane permittivity	$\epsilon_0\epsilon_m$ (F m^{-1})	7.6×10^{-10}	7.8×10^{-10}	4.4×10^{-11}	4.4×10^{-11}
Membrane, conductivity	σ_m (S m^{-1})	3×10^{-7}	10^{-6}	5×10^{-7}	5×10^{-7}
External medium permittivity	$\epsilon_0\epsilon_e$ (F m^{-1})	7.1×10^{-10}	7.1×10^{-10}	7×10^{-10}	7×10^{-10}
External medium conductivity	σ_e (S m^{-1})	0.75	0.012	0.2	0.2
Membrane Young modulus	Y_m (Pa)		500	19×10^{6}	19×10^{6}
Cytoplasm Young modulus	Y_c (Pa)		10^3	10^3	10^3
Membrane shear modulus	G_m (Pa)		1.5×10^3		
Membrane viscous relaxation time	$\tau_{rel,m}$ (s)		0.1		
Nucleus membrane thickness	d_{nm} (m)	40×10^{-9}			
Nucleus membrane conductivity	σ_{nm} (Sm^{-1})	6×10^{-3}			
Nucleus membrane permittivity	$\epsilon_0\epsilon_{nm}$ (Fm^{-1})	4.6×10^{-10}			
Nucleus conductivity	σ_n (Sm^{-1})	1.35			
Nucleus permittivity	$\epsilon_0\epsilon_n$ (Fm^{-1})	4.6×10^{-10}			

simulations.[6,22,23,106] The reader is also referred to other sources that describe the physical parameters used in the FE analysis of biological cells exposed to electric fields.[4,12,13,15,26,28,48,49,58]

DATA AVAILABILITY

The data that support the findings of this work are available from the corresponding author upon reasonable request.

REFERENCES

[1]C. Verdier, J. Etienne, A. Duperray, and L. Preziosi, "Review: Rheological properties of biological materials," C. R. Phys. **10**, 790–811 (2009); M. Luckey, Membrane Structural Biology (Cambridge University Press, 2008).

[2]H. P. Schwan, Adv. Biol. Med. Phys. **5**, 147 (1957); "Historical Review, State of the Art, Open Problems," in *Interactions Between Electromagnetic Fields and Cells*, edited by A. Chiabrera, C. Nicolini, and H. P. Schwan (Plenum Press, New York, 1985), pp. 1–18; *Electroporation and Electrofusion in Cell Biology* (Plenum Press, 1989).

[3]K. R. Foster and H. P. Schwan, Crit. Rev. Biomed. Eng. **17**, 25 (1989); H. Pauly and H. P. Schwan, Z. Naturforsch. B **14**, 125 (1959); in *Handbook of Biological Effects of Electromagnetic Fields*, edited by C. Polk and E. Postow (CRC Press, New York, 1996), pp. 25–102.

[4]T. Kotnik, G. Pucihar, D. Miklavčič *et al.*, "The cell in the electric field," in *Clinical Aspects of Electroporation*, edited by S. T. Kee (Springer Verlag, 2011); T. Kotnik and D. Miklavčič, "Theoretical evaluation of voltage inducement on internal membranes of biological cells exposed to electric fields," Biophys. J. 71, 868–877 (1996); M. Pavlin, V. Leben, and D. Miklavčič, "Electroporation in dense cell suspension: Theoretical and experimental analysis of ion diffusion and cell permeabilization," Biochim. Biophys. Acta Gen. Subj. 1770, 12–23 (2007); L. Rems and D. Miklavčič, "Tutorial: Electroporation of cells in complex materials and tissue," J. Appl. Phys. 119, 201101 (2016).

[5]E. C. Fear and M. A. Stuchly, "Modeling assemblies of biological cells exposed to electric fields," IEEE Trans. Biomed. Eng. **45**, 1259–1271 (1998).

[6]T. Murovec, D. C. Sweeney, E. Latouche, R. V. Davalos, and C. Brosseau, "Modeling of transmembrane potential in realistic multicellular structures before electroporation," Biophys. J. **111**, 2286–2295 (2016).

[7]M. Essone Mezeme, G. Pucihar, M. Pavlin, C. Brosseau, and D. Miklavčič, "A numerical analysis of multicellular environment for modeling tissue electroporation," Appl. Phys. Lett. **100**(1), 143701 (2012); M. Essone Mezeme, M. Kranjc, F. Bajd, I. Sersa, C. Brosseau, and D. Miklavčič, "Assessing how electroporation affects the effective conductivity tensor of biological tissues," Appl. Phys. Lett. **101**, 213702(1)–213702(4) (2012).

[8]T. J. Lewis, "Interfaces are the dominant feature of dielectrics at the nanometric level," IEEE Trans. Dielectr. Electr. Insul. **11**, 739–753 (2004); W. C. Chew and P. N. Sen, "Potential of sphere in an ionic solution in thin double layer approximation," J. Chem. Phys. **77**, 2042–2044 (1982); S. Genet, R. Costalat, and J. Burger, "The Influence of plasma membrane electrostatic properties on the stability of cell ionic composition," Biophys. J. **81**, 2442–2457 (2001).

[9]D. Shamoon, J. Dermol-Cerne, L. Rems, M. Rebersek, T. Kotnik, S. Lasquellec, C. Brosseau, and D. Miklavčič, "Assessing the electro-deformation and electropermeabilization of biological cells using a three dimensional finite element model," Appl. Phys. Lett. **114**, 063701–063701(5) (2019).

[10]K. A. DeBruin and W. Krassowska, "Modeling electroporation in a single cell. I. Effects of field strength and rest potential," Biophys. J. **77**, 1213–1224 (1999); "Modeling electroporation in a double cell. II. Effects of ionic concentrations" **77**, 1225–1233 (1999).

[11]Z. A. Levine and P. T. Vernier, "Life cycle of an electropore: Field-dependent and field-independent steps in pore creation and annihilation," J. Membr. Biol. **236**, 27–36 (2010); A. G. Pakhomov, J. F. Kolb, J. A. White, R. P. Joshi, S. Ziao, and K. H. Schoenbach, "Long-lasting membrane permeabilization in mammalian cells by nanosecond pulsed electric field (nsPEF)," Bioelectromagnetics **28**, 655–663 (2007); A. G. Pakomov, E. Gianulis, P. T. Vernier, I. Semenov, S. Xiao, and O. Pakhomova, "Multiple nanosecond electric pulses increase the number but not the size of long-lived nanopores in the cell membrane," Biochim. Biophys. Acta **1848**, 958–966 (2015).

[12]D. P. Tieleman, H. Leontiadon, A. E. Mark, and S.-J. Marrink, "Simulation of pore formation in lipid bilayers by mechanical stress and electric fields," J. Am. Chem. Soc. **125**, 6382–6383 (2003).

[13]D. C. Sweeney, T. A. Douglas, and R. V. Davalos, "Characterization of cell membrane permeability *in vitro*. Part II: Computational model of electroporation-mediated membrane transport," Technol. Cancer Res. Treat. **17**, 1–13 (2018).

[14]J. C. Weaver, K. T. Powell, R. A. Mintzer, H. Ling, and S. R. Sloan, "The electrical capacitance of bilayer membranes: The contribution of transient aqueous pores," Bioelectrochem. Bioenerg. **12**, 393–404 (1984).
[15]L. Mescia, M. A. Chiapperino, P. Bia, C. M. Lamacchia, J. Gielis, and D. Caratelli, "Design of electroporation process in irregularly shaped multicellular systems," Electronics **8**(1), 37 (2019).
[16]R. Pethig and G. Marks, "Applications of dielectrophoresis in biotechnology," Trends Biotechnol. **15**, 426–432 (1997).
[17]T. B. Jones, *Electromechanics of Particles* (Cambridge University Press, 2005).
[18]M. E. Gurtin, *An Introduction to Continuum Mechanics* (Academic Press, 1982).
[19]R. Pethig, *Dielectric and Electronic Properties of Biological Materials* (Wiley, New York, 1979); C. Gabriel, "Dielectric properties of biological materials," in *Bioengineering and Biophysical Aspects of Electromagnetic Fields*, edited by F. S. Barnes and B. Grenebaum (CRC Press, New York, 2006); K. R. Foster and H. P. Schwan, Crit. Rev. Biomed. Eng. **17**, 25 (1989).
[20]J. Preto, M. Pettini, and J. A. Tuszynski, "Possible role of electrodynamic interactions in long-distance biomolecular recognition," Phys. Rev. E **91**, 052710 (2015).
[21]E. Moeendarbary, L. Valon, M. Fritzsche, A. R. Harris, D. A. Moulding, A. J. Thrasher, E. Stride, L. Mahadevan, and G. T. Charras, "The cytoplasm of living cells behaves as a poroelastic material," Nat. Mater. **12**, 253–261 (2013).
[22]D. Shamoon, S. Lasquellec, and C. Brosseau, "A multiphysics analysis of the strain energy in multicellular environments," Appl. Phys. Lett. **115**, 043701 (2019).
[23]E. Sabri, S. Lasquellec, and C. Brosseau, "Electromechanical modeling of the transmembrane potential-dependent cell membrane capacitance," Appl. Phys. Lett. **117**, 043701 (2020).
[24]D. Shamoon, S. Lasquellec, and C. Brosseau, "Perspective: Towards understanding the multiscale description of cells and tissue by electromechanobiology," J. Appl. Phys. **123**, 240902 (2018); D. Shamoon, S. Lasquellec, and C. Brosseau, "Low-order statistics of the effective permittivity and electric field fluctuations in two-phase heterostructures," J. Appl. Phys. **122**, 044106 (2017); The latter paper provides a small N limit for the effective permittivity estimator, variance, and mean square error that is correct for an arbitrary two-phase heterostructure, where N is proportional to an internal length scale.
[25]T. Kotnik and D. Miklavčič, "Analytical description of transmembrane voltage induced by electric fields on spheroidal cells," Biophys. J. **79**, 670–679 (2000); U. van Rienen, J. Flehr, U. Schreiber, S. Schulze, U. Gimsa, W. Baumann, D. G. Weiss, J. Gimsa, R. Benecke, and H. W. Pau, "Electroquasistatic simulations in bio-systems engineering and medical engineering," Adv. Radio Sci. **3**, 39–49 (2005); Z. Lojewska, D. L. Farkas, B. Ehrenberg, and L. M. Loew, "Analysis of the effect of medium and membrane conductance on the amplitude and kinetics of membrane potentials induced by externally applied electric fields," Biophys. J. **56**, 121–128 (1989); J. Gimsa, M. Stubbe, and U. Gimsa, "A short tutorial contribution to impedance and AC-electrokinetic characterization and manipulation of cells and media: Are electric methods more versatile than acoustic and laser methods?," J. Electr. Bioimpedance **5**, 74–91 (2014).
[26]L. Rems, M. Tarek, M. Casciola, and D. Miklavčič, "Properties of lipid electropores II: Comparison of continuum-level modeling of pore conductance to molecular dynamics simulations," Bioelectrochemistry **112**, 112–124 (2016).
[27]R. Pethig, *Dielectric and Electronic Properties of Biological Materials* (Wiley, New York, 1979); C. Gabriel, "Dielectric properties of biological materials," in *Bioengineering and Biophysical Aspects of Electromagnetic Fields*, edited by F. S. Barnes and B. Grenebaum (CRC Press, New York, 2006).
[28]G. Pucihar, D. Miklavčič, and T. Kotnik, "A time-dependent numerical model of transmembrane voltage inducement and electroporation of irregularly shaped cells," IEEE Trans. Biomed. Eng. **56**, 1491–1501 (2009).
[29]J. C. Weaver, "Electroporation of biological membranes from multicellular to nano scales," IEEE Trans. Dielectr. Electr. Insul. **10**, 754–768 (2003).
[30]B. Varga, C. Fazakas, I. Wilhelm, I. A. Krizbai, Z. Szegletes, G. Váró, and A. G. Végh, "Elasto-mechanical properties of living cells," Biochem. Biophys. Rep. **7**, 303–308 (2016).
[31]M.-A. Meyers, P.-Y. Chen, A. Y.-M. Lin, and Y. Seki, "Biological materials: Structure and mechanical properties," Prog. Mater. Sci. **53**, 1–206 (2008).
[32]N. Wang, J. Butler, and D. Ingber, "Mechanotransduction across the cell surface and through the cytoskeleton," Science **260**, 1124 (1993).
[33]A. R. Dunn and A. Price, "Energetics and forces in living cells," Phys. Today **68**, 27 (2015).
[34]A. M. Handorf, Y. Zhou, M. A. Halanski, and W.-J. Li, "Tissue stiffness dictates development, homeostasis, and disease progression," Organogenesis **11**, 1–15 (2015).
[35]N. Bonakdar, R. Gerum, M. Kuhn, M. Spörrer, A. Lippert, W. Schneider, K. E. Aifantis, and B. Fabry, "Mechanical plasticity of cells," Nat. Mater. **15**, 1090–1094 (2016).
[36]J. Eyckmans, T. Boudou, X. Yu, and C. S. Chen, "A hitchhiker's guide to mechanobiology," Dev. Cell **21**, 35–47 (2011); E. Goldberg, C. Suarez, M. Alfonso, J. Marchese, A. Soba, and G. Marshall, "Cell membrane electroporation modeling: A multiphysics approach," Bioelectrochemistry **124**, 28–39 (2018).
[37]L. Yu and Y. Sheng, "Effect of object 3D shape on the viscoelastic testing in optical tweezers," Opt. Express **23**, 6020–6028 (2015); T. Klöppel and W. A. Wall, "A novel two-layer, coupled finite element approach for modeling the nonlinear elastic and viscoelastic behavior of human erythrocytes," Biomech. Model. Mechanobiol. **10**, 445–459 (2011).
[38]B. Alberts, J. H. Wilson, and T. Hunt, in *Molecular Biology of the Cell*, 5th ed. (Garland Science, New York, 2008).
[39]D. E. Ingber, "Tensegrity I. Cell structure and hierarchical systems biology," J. Cell Sci. **116**, 1157 (2003); D. E. Ingber, N. Wang, and D. Stamenovic, "Tensegrity, cellular biophysics, and the mechanics of living systems," Rep. Prog. Phys. **77**, 046603 (2014).
[40]L. D. Mosgaard, K. A. Zecchi, and T. Heimburg, "Mechano-capacitive properties of polarized membranes," Soft Matter **11**, 7899–7910 (2015).
[41]U. Zimmermann and G. Küppers, "Cell fusion by electromagnetic waves and its possible relevance for evolution," Naturwissenchaften **70**, 568–569 (1983).
[42]J. H. Kroeger, D. Vernon, and M. Grant, "Curvature-driven pore growth in charged membranes during charge-pulse and voltage-clamp experiments," Biophys. J. **96**, 907–916 (2009).
[43]There have been textbook materials on the viscoelasticity of biological structures for more than 30 years including a complement of both physical and biological research methods, see, e.g., R. G. Larson, *The Structure and Rheology of Complex Fluids* (Oxford University Press, New York, 1999); Y. C. Fung, in *Biomechanics. Mechanical Properties of Living Tissues*, 2nd ed. (Springer Verlag, New York, 1993); A. Chauvière, L. Preziosi, and C. Verdier, *Cell Mechanics From Single Scale-Based Models to Multiscale Modeling* (Chapman & Hall/CRC, 2009).
[44]K. E. Kasza, A. C. Rowat, J. Liu, T. E. Angelini, C. P. Brangwynne, G. H. Koenderink, and D. A. Weitz, "The cell as a material," Curr. Opin. Cell Biol. **19**, 101 (2007).
[45]M. Tarek, "Membrane electroporation: A molecular dynamics simulation," Biophys. J. **88**, 4045–4053 (2005); L. Delemotte and M. Tarek, "Molecular dynamics simulations of lipid membrane electroporation," J. Membr. Biol. **245**, 531543 (2012); M. Casciola and M. Tarek, "A molecular insight into the electrotransfer of small molecules through electropores driven by electric fields," Biochim. Biophys. Acta Biomembr. **1858**, 2278–2228 (2016).
[46]R. A. Böckmann, B. L. de Groot, S. Kakorin, E. Neumann, and H. Grubmüller, "Kinetics, statistics, and energetics of lipid membrane electroporation studied by molecular dynamics simulations," Biophys. J. **95**, 1837–1850 (2008).
[47]M. J. Ziegler and P. T. Vernier, "Interface water dynamics and porating electric fields for phospholipid bilayers," J. Chem. Phys. B **112**, 17003–17003 (2008).
[48]K. Asami, "Dielectric dispersion in biological cells of complex geometry simulated by the three-dimensional finite difference method," J. Phys. D **39**, 492–499 (2006); K. Asami, T. Hanai, and N. Koizumi, "Dielectric approach to suspensions of ellipsoidal particles covered with a shell in particular reference to biological cells," Jpn. J. Appl. Phys. **19**, 359–365 (1980); K. Asami, "Characterization of heterogeneous systems by dielectric spectroscopy," Prog. Polym. Sci. **27**, 1617–1659 (2002); K. Asami, "Simulation for the dielectric images of single biological cells obtained using a scanning dielectric microscope," J. Phys. D **41**, 085501 (2008).
[49]L. Rems, M. Ušaj, M. Kandušer, M. Reberšek, D. Miklavčič, and G. Pucihar, "Cell electrofusion using nanosecond electric pulses," Sci. Rep. **3**, 3382 (2013).

[50]M. Yu and H. Lin, "Modelling transport across the electroporated membrane," in *Handbook of Electroporation*, edited by D. Milklavcic (Springer, 2016).
[51]R. S. Eisenberg and R. T. Mathias, "Structural analysis of electrical properties," Crit. Rev. Bioeng. **4**, 203–232 (1980).
[52]C. T. Everitt and D. A. Haydon, "Electrical capacitance of a lipid membrane separating two aqueous phases," J. Theor. Biol. **18**, 371–379 (1968).
[53]K. C. Smith, J. C. Neu, and W. Krassowska, "Model of creation and evolution of stable macropores for DNA delivery," Biophys. J. **86**, 2813–2826 (2004).
[54]J. C. Neu and W. Krassowska, "Asymptotic model of electroporation," Phys. Rev. E **59**, 3471–3482 (1999).
[55]A. Barnett and J. C. Weaver, "Electroporation: A unified quantitative theory of reversible electrical breakdown and mechanical rupture in artificial planar bilayer membranes," Bioelectrochem. Bioenerg. **25**, 163–182 (1991).
[56]D. A. Stewart, T. R. Gowrishankar, and J. C. Weaver, "Transport lattice to describing cell electroporation use of a local asymptotic model," IEEE Trans. Plasma Sci. **32**, 1696–1708 (2004); T. R. Gowrishankar and J. C. Weaver, "An approach to electrical modeling of single and multiple cells," Proc. Natl. Acad. Sci. U.S.A. **100**, 3203–3208 (2003).
[57]A. Ramos, "Effect of the electroporation in the field calculation in biological tissues," Artif. Organs **29**, 510–513 (2005); A. Ramos, A. Raizer, and L. B. Marques, "A new computational approach for electrical analysis of biological tissues," Bioelectrochemistry **59**, 73–84 (2003).
[58]S. Sundelacruz, M. Levin, and D. L. Kaplan, "Role of membrane potential in the regulation of cell proliferation and differentiation," Stem Cell Rev. Rep. **5**, 231–246 (2009); R. Nuccitelli, "Endogenous electric fields in embryos during development, regeneration and wound healing," Radiat. Prot. Dosim. **106**, 375–383 (2003); C. D. McCaig, A. M. Rajnicek, B. Song, and M. Zhao, "Controlling cell behavior electrically: Current views and future potential," Physiol. Rev. **85**, 943–978 (2005).
[59]J. T. Sengel and M. I. Wallace, "Imaging the dynamics of individual electropores," Proc. Natl. Acad. Sci. U.S.A. **113**, 5281–5286 (2016).
[60]A. C. Scott, "The electrophysics of a nerve fiber," Rev. Mod. Phys. **47**, 487 (1975).
[61]R. P. Joshi and K. H. Schoenbach, "Electroporation dynamic in biological cells subjected to ultrafast pulses: A numerical simulation study," Phys. Rev. E **62**, 1025–1033 (2000); K. H. Schoenbach, R. P. Joshi, J. R. Kolb, N. Chen, M. Stacey, P. F. Blackmore, E. S. Buescher, and S. J. Beebe, "Ultrashort electrical pulses open a new gateway into biological cells," Proc. IEEE **92**, 1122–1137 (2004).
[62]H. Isambert, "Understanding the electroporation of cells and artificial bilayer membranes," Phys. Rev. Lett. **80**, 3404 (1998).
[63]R. S. Son, T. R. Gowrishankar, K. C. Smith, and J. C. Weaver, "Modeling a conventional electroporation pulse train: Decreased pore number, cumulative calcium transport and an example of electrosensitization," IEEE Trans. Biomed. Eng. **63**, 2016571 (2016).
[64]J. C. Weaver, K. C. Smith, A. T. Esser, R. S. Son, and T. R. Gowrishankar, "A brief overview of electroporation pulse strength-duration space: A region where additional intracellular effects are expected," Biolectrochem. **87**, 236–243 (2012).
[65]L. D. Landau and E. M. Lifshitz, *Electrodynamics of Continuous Media* (Pergamon Press, New York, 1984); D. T. Edmonds, *Electricity and Magnetism in Biological Systems* (Oxford University Press, 2001).
[66]R. Lisin, B. Z. Ginzburg, M. Schlesinger, and Y. Feldman, "Time domain dielectric spectroscopy study of human cells I," Biochim. Biophys. Acta **1280**, 34–40 (1996).
[67]E. Gongadze, A. Velikonja, S. Perutkova, P. Kramar, A. Macek-Lebar, V. Kralj-Iglič, and A. Iglič, "Ions and watermolecules in an electrolyte solution in contact with charged and dipolar surfaces," Electrochim. Acta **126**, 42–60 (2014); M. V. Fedorov, N. Georgi, and A. A. Kornyshev, "Double layer in ionic liquids: The nature of the camel shape of capacitance," Electrochem. Commun. **12**, 296–299 (2010); E. Gongadze and A. Iglič, "Asymmetric size of ions and orientational ordering of water dipoles in electric double layer model: An analytical mean-field approach," Electrochim. Acta **178**, 541–545 (2015); Y. Zhang and J. Huang, "Treatment of ion-size asymmetry in lattice-gas models for electrical double layer," J. Phys. Chem. C **122**, 28652–28664 (2018).
[68]K. Kinosita and T. Y. Tsong, "Formation and resealing of pores of controlled sizes in human erythrocyte membrane," Nature **268**, 438–441 (1977); M. Hibino, M. Shigemori, H. Itoh, K. Nagayama, and K. Kinosita, "Membrane conductance of an electroporated cell analyzed by submicrosecond imaging of transmembrane potential," Biophys. J. **59**, 209–220 (1991); K. Kinosita, I. Ashikawa, N. Saita, H. Yoshimura, H. Itoh, K. Nagayama, and A. Ikegami, "Electroporation of cell membrane visualized under a pulsed-laser fluorescence microscopy," Biophys. J. **53**, 1015–1019 (1988); M. Hibino, H. Itoh, and K. Kinosita, "Time courses of cell electroporation as revealed by submicrosecond imaging of transmembrane potential," Biophys. J. **64**, 1789–1800 (1993).
[69]T. Murovec and C. Brosseau, "Spectral fingerprint of electrostatic forces between biological cells," Phys. Rev. E **92**, 042717 (2015).
[70]L. D. Mosgaard, K. A. Zecchi, and T. Heimburg, "Mechano-capacitive properties of polar membranes," Soft Matter **11**, 7899 (2015); L. D. Mosgaard, K. A. Zecchi, T. Heimburg, and R. Budvytyte, "The effect of the nonlinearity of the response of lipid membranes to voltage perturbations on the interpretation of its electrical properties," Membranes **5**, 495 (2015).
[71]O. Alvarez and R. Latorre, "Voltage-dependent capacitance in lipid bilayers made from monolayers," Biophys. J. **15**, 77 (1975).
[72]T. Heimburg, "The capacitance and electromechanical coupling of lipid membranes close to transitions. The effect of electrostriction," Biophys. J. **103**, 918 (2012); T. Heimburg, Thermal Biophysics of Membranes (Wiley VCH, Berlin, Germany, 2007).
[73]S. Roy, W. E. Brownell, and A. A. Spector, "Modeling electrically active viscoelastic membranes," PLoS ONE **7**, 37667 (2012).
[74]Q. Hu, R. P. Joshi, and A. Beskok, "Mode study of electroporation effects on the dielectrophoretic response of spheroidal cells," J. Appl. Phys. **106**, 024701 (2009).
[75]B. I. Morshed, M. Shams, and T. Mussivand, "Deriving an electric circuit equivalent model of cell membrane pores in electroporation," Biophys. Rev. Lett. **08**, 21–32 (2013).
[76]J. Teissié and M. P. Rols, "An experimental evaluation of the critical potential difference inducing cell membrane electropermeabilization," Biophys. J. **65**, 409–413 (1993).
[77]P. F. Salipante, R. L. Knorr, R. Dimova, and P. M. Vahovska, "Electrodeformation method for measuring the capacitance of bilayer membranes," Soft Matter **8**, 3810–3816 (2012); R. Dimova, K. A. Riske, S. Aranda, N. Bezlyepkina, R. L. Knorr, and R. Liposky, "Giant vesicles in electric fields," Soft Matter **3**, 817–827 (2007); R. Dimova, "Vesicles in electric fields: Some novel aspects of membrane behavior," Soft Matter **5**, 3201–3212 (2009).
[78]D. Needham and R. M. Hochmuth, "Electro-mechanical permeabilization of lipid vesicles," Biophys. J. **55**, 1001–1009 (1989).
[79]E. Neumann and K. Rosenheck, "Permeability changes induced by electric impulses in vesicular membranes," J. Membr. Biol. **10**, 279–290 (1972).
[80]J. Akinlaja and F. Sachs, "The breakdown of cell membranes by electrical and mechanical stress," Biophys. J. **75**, 247–254 (1998); I. G. Abiror, V. B. Arakelyan, L. V. Chernomordik, Y. A. Chizmadzhev, V. F. Pastushenko, and M. R. Tarasevich, "Electric breadown of bilayer lipid membranes I. The main experimental facts and their qualitative discussion," Bioelectrochem. Bioenerg. **6**, 37–52 (1979).
[81]M. Fošnarič, V. Kralj-Iglič, K. Bohinc, A. Iglič, and S. May, "Stabilization of pores in lipid bilayers by anisotropic inclusions," J. Phys. Chem. B **107**, 12519–12526 (2003).
[82]J. C. Weaver and Y. A. Chizmadzhev, "Theory of electroporation: A review," Bioelectrochem. Bioenerg. **41**, 135 (1996); C. Chen, S. W. Smye, M. P. Robinson, and J. Evans, "Membrane electroporation theories: A review," Med. Biol. Eng. Comput. **44**, 5 (2006); J. Teissié, M. Golzio, and M. Rols, "Mechanisms of cell membrane electropermeabilization: A minireview of our present (lack of?) knowledge," Biochim. Biophys. Acta, Gen. Subj. **1724**, 270–160 (2005).
[83]W. Krassowska and P. D. Filev, "Modelling electroporation in a single cell," Biophys. J. **92**, 404–417 (2007).
[84]K. DeBruin and W. Krassowska, "Electroporation and shock-induced transmembrane potential in a cardiac fiber during defribillation strength shocks," Ann. Biomed. Eng. **26**, 584–596 (1998).

[85]A. Barnett, "The current-voltage relation of an aqueous pore in a lipid bilayer membrane," Biochim. Biophys. Acta **1025**, 10–14 (1990).
[86]R. W. Glaser, S. L. Leikin, L. V. Chernomordik, V. F. Pastushenko, and A. I. Sokirko, "Reversible electrical breakdown of lipid bilayers: Formation and evolution of pores," Biochim. Biophys. Acta **940**, 275–287 (1988).
[87]B. V. Derjaguin, *Theory of Stability of Colloids and Thin Films* (Springer, 1989).
[88]U. Zimmermann, G. Pilwat, and F. Riemann, "Dielectric breakdown of cell membranes," Biophys. J. **14**, 881–899 (1974).
[89]I. G. Abidor, V. B. Arakelyan, and L. V. Chernomordik, "Electric breakdown of bilayer membranes: I. The main experimental facts and their qualitative discussion," Bioelectrochem. Bioenerg. **6**, 37–52 (1979).
[90]J. C. Weaver and R. A. Mintzer, "Decreased bilayer stability due to transmembrane potentials," Phys. Lett. A **86**, 57–59 (1981).
[91]P. Deng, Y.-K. Lee, R. Lin, and T.-Y. Zhang, "Nonlinear electro-mechanobiological behavior of cell membrane during electroporation," Appl. Phys. Lett. **101**, 05372 (2012).
[92]H. Shagoshtasbi, P. Deng, and Y.-K. Lee, "A nonlinear size-dependent equivalent circuit model for single-cell electroporation on microfluidic chips," J. Lab. Autom. **20**, 481–490 (2015).
[93]D. Voyer, A. Silve, L. M. Mir, R. Scoretti, and C. Poignard, "Dynamical modeling of tissue electroporation," Bioelectrochemistry **119**, 98–110 (2018); M. Leguébe, A. Silve, L. M. Mir, and C. Poignard, "Conducting and permeable states of cell membrane submitted to high voltage pulses. Mathematical and numerical studies validated by the experiments," J. Theor. Biol. **360**, 83–94 (2014).
[94]R. E. Neal II, P. A. Garcia, J. L. Robertson, and R. V. Davalos, "Experimental characterization and numerical modeling of tissue electrical conductivity during pulsed electric fields for irreversible electroporation treatment planning," IEEE Trans. Biomed. Eng. **59**, 1076–1085 (2012).
[95]S. P. Bhonsle, C. B. Arena, D. C. Sweenery, and R. V. Davalos, "Mitigation of impedance changes due to electroporation therapy using bursts of high-frequency bipolar pulses," Biomed. Eng. Online **14**, S3 (2015); S. H. Strogatz, "Exploring complex networks," Nature **410**, 268–276 (2001).
[96]F. Qian, S. Ermilov, D. Murdock, W. E. Brownell, and B. Anvari, "Combining optical tweezers and patch clamp for studies of cell membrane electromechanics," Rev. Sci. Instrum. **75**, 2937–2942 (2004); B. E. Henslee, A. Morss, X. Hu, G. P. Lafyatis, and L. J. Lee, "Electroporation dependence on cell size: Optical tweezers study," Anal. Chem. **83**, 3998–4003 (2011).
[97]S. M. White and T. E. Thompson, "Capacitance, area, and thickness variations in thin lipid films," Biochim. Biophys. Acta **323**, 7–22 (1973).
[98]A. Di Biasio, L. Ambrosone, and C. Cametti, "Numerical simulation of dielectric spectra of aqueous suspensions of non-spheroidal differently shaped biological cells," J. Phys. D: Appl. Phys. **42**, 025401 (2009); M. Essone Mezeme and C. Brosseau, "Simulation of a toy model of cylindrical cells submitted to nonionizing electromagnetic field: Effect of membrane cell disruption," J. Appl. Phys. **107**, 014701 (2010).
[99]B. E. Henslee, A. Morss, X. Hu, G. P. Lafyatis, and L. J. Lee, "Electroporation dependence on cell size: An optical tweezers study," Anal. Chem. **83**, 3998–4003 (2011).
[100]W. Liang, Y. Zhao, L. Liu, Y. Wang, W. J. Li, and G.-B. Lee, "Determination of cell membrane capacitance and resistance via optically induced electrokinetics," Biophys. J. **113**, 1531–1539 (2017).
[101]P. J. Canatella and M. R. Prausnitz, "Prediction and optimization of gene transfection and drug delivery by electroporation," Gene Ther. **8**, 1464–1469 (2001); P. J. Canatella, M. M. Black, D. M. Bonnichsen, and M. R. Prausnitz, "Tissue electroporation: Quantification and analysis of heterogeneous transport in multicellular environments," Biophys. J. **86**, 3260–3268 (2004).
[102]G. Thrivikraman, S. K. Boda, and B. Basu, "Unraveling the mechanistic effects of electric field stimulation towards directing stem cell fate and function: A tissue engineering perspective," Biomaterials **150**, 60–86 (2018); C. Chen, X. Bai, Y. Ding, and I. S. Lee, "Electrical stimulation as a novel tool for regulating cell behavior in tissue engineering," Biomater. Res. **23**, 1–12 (2019); R. Balint, N. J. Cassidy, and S. H. Cartmell, "Electrical stimulation: A novel tool for tissue engineering," Tissue Eng. Part B **19**, 48–57 (2013).
[103]T. Murovec and C. Brosseau, "Numerical simulation of the sign switching of the electrostatic force between charged conducting particles from repulsive to attractive," J. Appl. Phys. **116**, 214902 (2014); "Does like attract like?," Appl. Phys. Lett. **105**, 054101 (2014); "Spectral fingerprint of electrostatic forces between biological cells," Phys. Rev. E **92**, 042717 (2015).
[104]D. Shao, W.-J. Rappel, and H. Levine, "Computational model for cell morphodynamics," Phys. Rev. Lett. **105**, 108104 (2010).
[105]A. Anderson and K. Rejniak, *Single Cell-Based Models in Biology and Medecine* (Birkhäuser, Basel, 2007).
[106]E. Sabri and C. Brosseau, "Proximity-induced electrodeformation and membrane capacitance coupling between cells" (unpublished).
[107]R. Susil, D. Semrov, and D. Miklavčič, "Electric field induced transmembrane potential depends on cell density and organization," Electro-Magnetobiology **17**, 391–399 (1998); P. A. Garcia, R. V. Davalos, and D. Miklavčič, "A numerical investigation of the electric and thermal cell kill distributions in electroporation-based therapies in tissues," PLoS One **9**, e103083 (2014).
[108]D. G. Lorich, C. T. Brighton, R. Gupta, J. R. Corsetti, S. E. Levine, I. D. Gelb, R. Seldes, and S. R. Pollack, "Biochemical pathway mediating the response of bone cells to capacitive coupling," Clin. Orthop. Relat. Res. **350**, 246–256 (1998); S. Krueger, S. Achilles, J. Zimmermann, T. Tischer, R. Bader, and A. Jonitz-Heincke, "Re-differentiation capacity of human chondrocytes *in vitro* following electrical stimulation with capacitively coupled fields," J. Clin. Med. **8**, 1771 (2019).
[109]S. B. Knightley, T. F. Blitchington, B. C. Hill, A. O. Grant, W. M. Smith, T. C. Pilkington, and R. E. Ideker, "Optical measurements of transmembrane potential changes during electric field stimulation of ventrical cells," Circ. Res. **72**, 255–270 (1993); L. M. Loew, "Voltage sensitive dyes: Measurement of membrane potentials induced by Dc and AC electric fields," Bioelectromagnetics Suppl. **1**, 179–189 (1992); V. Montana, D. L. Farkas, and L. M. Loew, "Dual-wavelength ratiometric fluorescence measurements of membrane-potential," Biochemistry **28**, 4536–4539 (1989); D. Gross, L. M. Loew, and W. Webb, "Optical imaging of cell membrane potential changes induced by applied electric fields," Biophys. J. **50**, 339–348 (1986).
[110]U. Zimmermann, "Electric field-mediated fusion and related electrical phenomena," Biochim. Biophys. Acta **694**, 227 (1982); U. Zimmermann and G. A. Neil, Electromanipulation of Cells (CRC Press, 1996); E. Neumann, M. Schaefer-Ridder, and Y. Wang, "Gene transfer into mouse lyoma cells by electroporation in high electric fields," EMBO J. **1**, 841–277 (1982); J. Eyckmans, T. Boudou, and X. Yu, "A hitchhiker's guide to mechanobiology," Dev. Cell **21**, 35–47 (2011); P. Katira, M. H. Zama, and R. T. Bonnecaze, "How changes in cell mechanical properties induce cancerous behavior," Phys. Rev. Lett. **108**, 028103 (2012); A. Ivorra and B. Rubinsky, "*In vivo* electrical impedance measurements during and after electroporation of rat liver," **70**, 287–295 (2007); T. Malecka-Massalska, R. Mlak, A. Smoleh, A. Brzozowska, W. Surtel, and K. Morshed, "Capacitance of membrane as a prognostic indicator of survival in head and neck cancer," PLoS One **11**, e0165809 (2016).
[111]M. L. Pall, "Electromagnetic fields act via activation of voltage-gated calcium channels to produce beneficial or adverse effects," J. Cell. Mol. Med. **17**, 958–965 (2013); C. Poignard, A. Silve, F. Campion, L. M. Mir, O. Saut, and L. Schwartz, "Ion fluxes, transmembrane potential, and osmotic stabilization: A new dynamic electrophysiological model for eukaryotic cells," Eur. Biophys. J. **40**, 235–246 (2011); P. E. Boukany, A. Morss, W.-C. Liao, B. Henslee, H. Jung, X. Zhang, B. Yu, X. Wang, Y. Wu, L. Li, K. Gao, X. Hu, X. Zhao, O. Hemminger, W. Lu, G. P. Lafyatis, and L. James Lee, "Nanochannel electroporation delivers precise amounts of biomolecules into living cells," Nat. Nanotechnol. **6**, 747–754 (2011); A. J. Ellingsrud, A. Solbra, G. T. Einevoll, G. Halnes, and M. E. Rognes, "Finite element simulation of ionic electrodiffusion in cellular geometries," arXiv:1911.03211, 2019.
[112]J. Selberg, M. Gomez, and M. Rolandi, "The potential for convergence between synthetic biology and bioelectronics," Cell Syst. **7**, 231–244 (2018).